

## CHAPTER 5

### RESULTS FROM CONDUCTIVITY STUDIES BY EIS

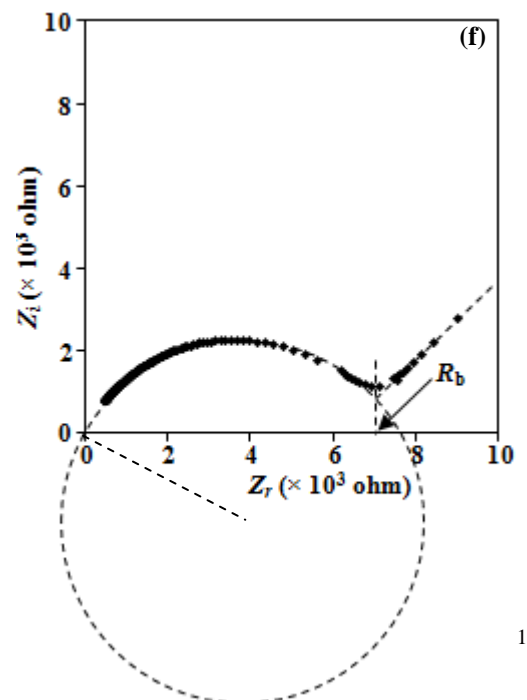
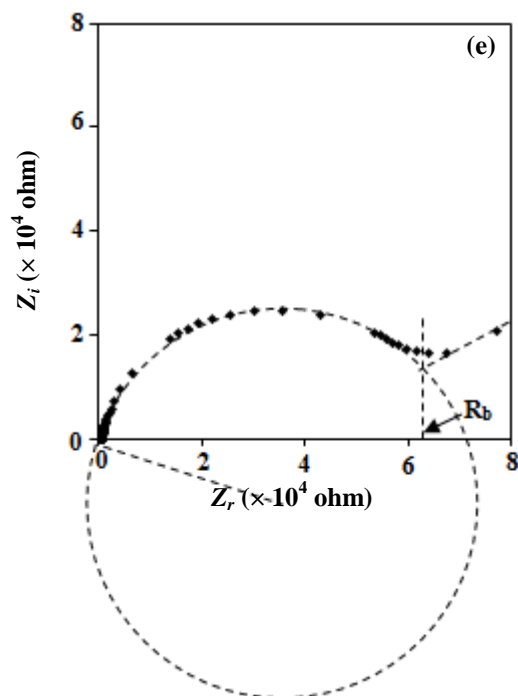
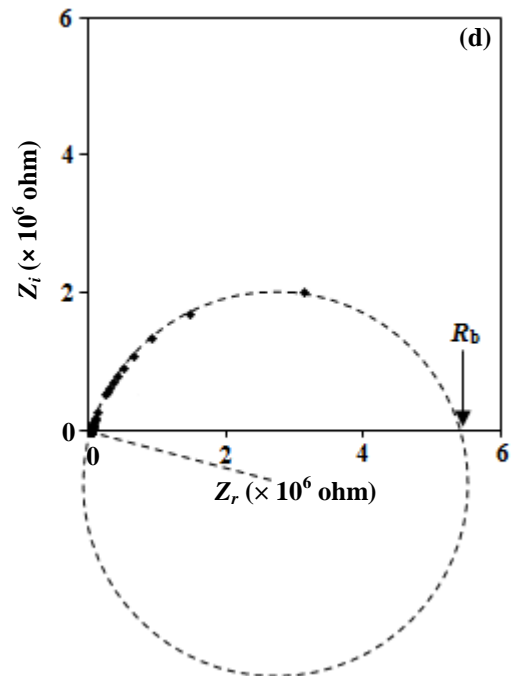
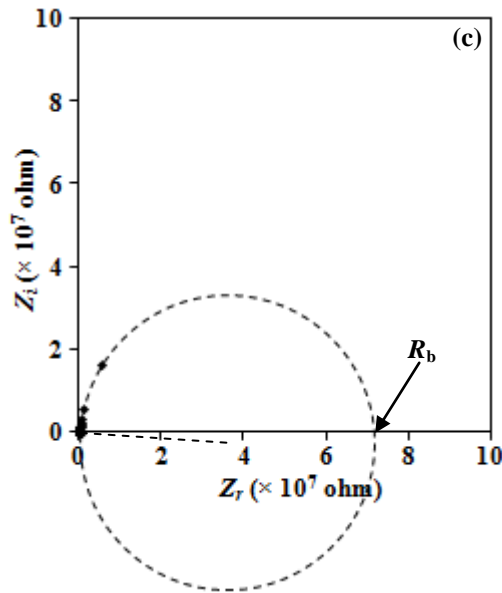
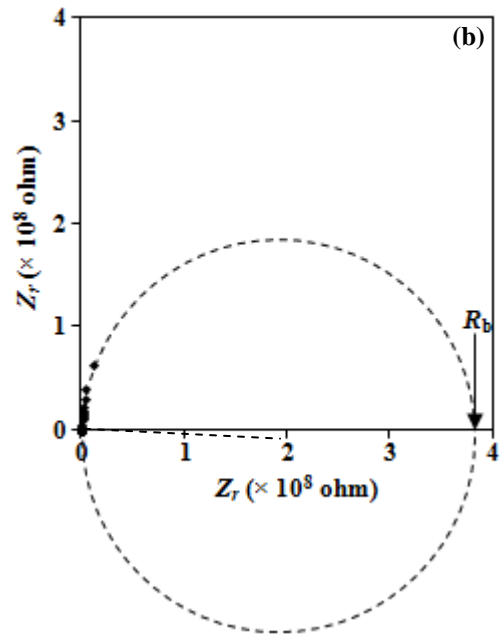
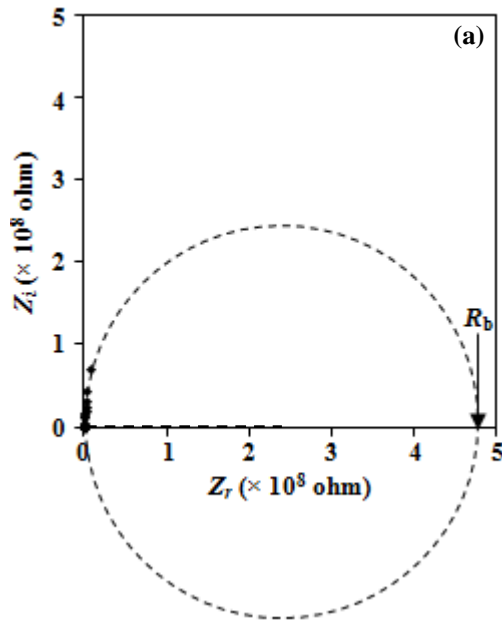
#### 5.1 Introduction

Ionic conductivity is one of the most crucial properties of polymer electrolytes. This is because polymer electrolytes possessing sufficiently high ionic conductivity are required for application in electrochemical devices. The higher the ionic conductivity, the more the charge that can be transported through a polymer electrolyte. Ionic conductivity is produced from the transport of charge carriers in the form of cations and anions which are present in the polymer electrolytes. In this chapter, the effect of the addition of various wt.% of LiTf on the ionic conductivity of PEMA/PVdF–HFP blend composition was studied. Upon optimization of the best polymer blend–salt composition with adequate ionic conductivity and good mechanical stability, the effect of carbonate based–plasticizer (i.e. EC and PC) and imidazolium based–ionic liquid (i.e. BMII and BMITf) was studied using EIS.

#### 5.2 Solid PEMA/PVdF–HFP–LiTf Polymer Electrolyte System

##### 5.2.1 Composition Dependence Conductivity Studies

For PEMA/PVdF–HFP–LiTf system, the conducting ions are  $\text{Li}^+$  and  $\text{Tf}^-$  ions which are dissociated from LiTf salt. Figure 5.1 depicts the Nyquist plots of PEMA/PVdF–HFP containing varied LiTf contents at room temperature.



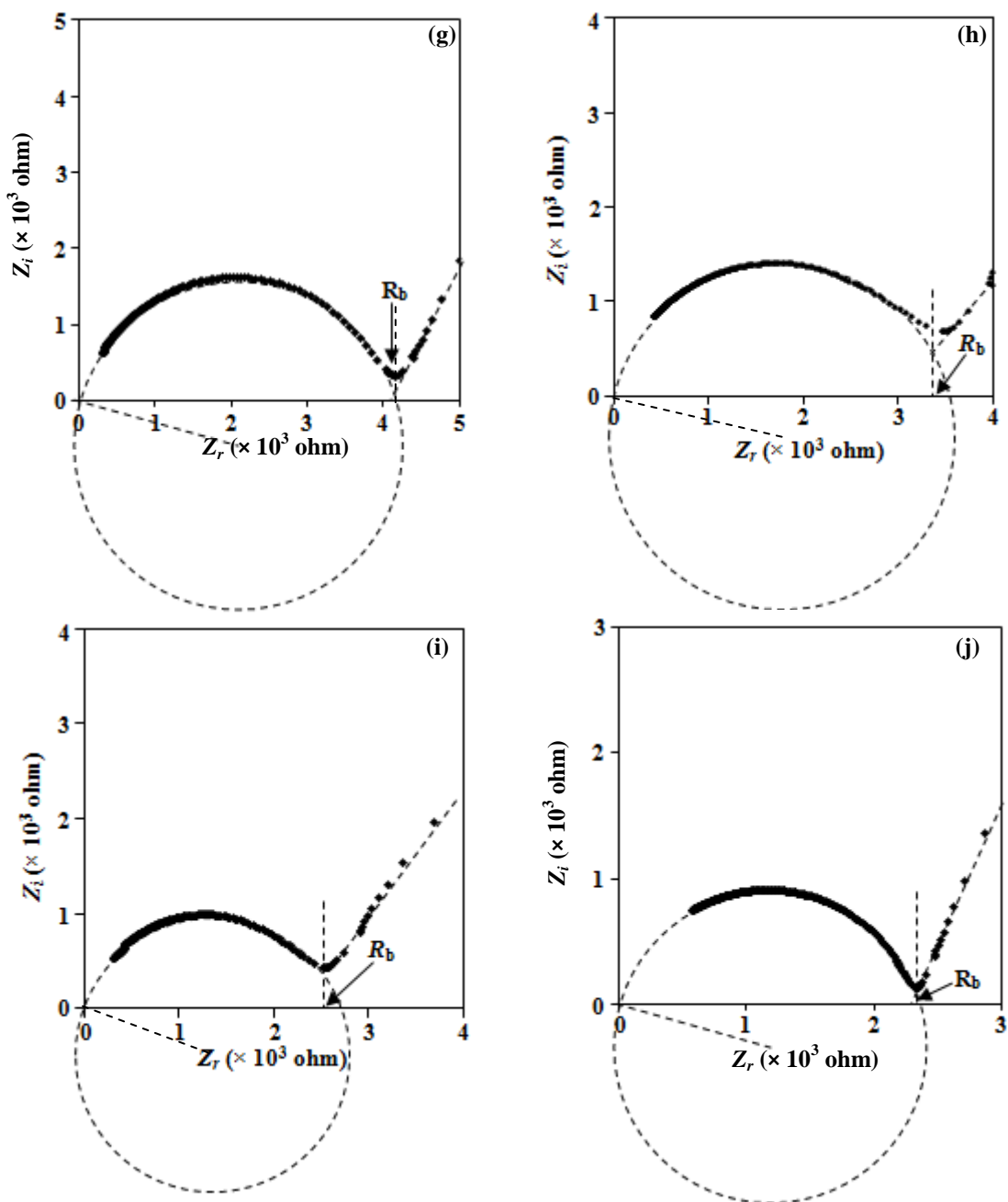


Figure 5.1 Nyquist plots of (a) S-0, (b) S-5, (c) S-10, (d) S-12.5, (e) S-15, (f) S-20, (g) S-25, (h) S-30, (i) S-35, (j) S-40 films

Upon increasing addition of LiTf, the Nyquist plots were observed to change from an incomplete semicircle in S-5, S-10 and S-12.5 samples (Figure 5.1 (b) to (d)) to a semicircle with a spike in samples containing contents of LiTf higher than 12.5 wt.% (Figure 5.1 (e) to (j)). If a material is purely capacitive with no charge transfer at the electrodes, a straight line parallel to the imaginary impedance axis would be

produced. The inclined spike observed at lower frequencies is due to the presence of double layer at the electrode–electrolyte interface. The incomplete semicircle observed in S–5, S–10 and S–12.5 suggests the presence of a capacitive component at higher frequencies [Raphael et al., 2010].

For samples containing 15 wt.% and above of LiTf, each Nyquist plot shows a depressed semicircle at high frequency and a spike at low frequency. The depressed semicircle with its centre lying below the real axis indicates non–Debye process which suggests the presence of distributed relaxation times due to distributed elements in the system [Gray, 1997]. The semicircle and the spike represent the bulk and charge transfer processes, respectively. The  $R_b$  value for S–0, S–5, S–10 and S–12.5 was obtained by the taking the intercept of the extrapolated incomplete circle with the real axis. For samples containing LiTf content higher than 12.5 wt.%, the intercept of the semicircle at higher frequencies with the spike at lower frequencies was used to obtain  $R_b$  value. It could be observed that the bulk resistance,  $R_b$  decreased continuously from the order of  $10^8$  ohm in S–0 to  $10^3$  ohm in S–40. To verify the analysis taken, the impedance data were converted into the admittance (A) formalism and the value of  $R_b$  obtained from the admittance plots are in reasonable agreement with that obtained from the Nyquist plots. Using equation (3.1), the ionic conductivity,  $\sigma$  at 298 K was calculated for PEMA/PVdF–HFP–LiTf samples. The plot of ionic conductivity against amount of LiTf is shown in Figure 5.2.

S–0 exhibits  $\sigma$  value of  $1.82 \times 10^{-12}$  S cm<sup>-1</sup> at room temperature. The ionic conductivity increased five orders to  $10^{-7}$  S cm<sup>-1</sup> with increasing LiTf content up to 40 wt.%. The ionic conductivities of PEMA/PVdF–HFP–LiTf system are listed in Table 5.1. Upon addition of 40 wt. % and more of LiTf salt, the mechanical stability of the

films obtained decreased and the films became soft which could easily tear. Although ionic conductivity is an important factor in polymer electrolytes, dimensional stability of the films also determines the suitability of the electrolyte to be used for practical applications. Hence, films with 40 wt.% and more of LiTf were not considered for further experiments and the composition of S-30 was chosen as the optimized composition due to its reasonable ionic conductivity of  $2.87 \times 10^{-7} \text{ S cm}^{-1}$  and good mechanical stability at room temperature.

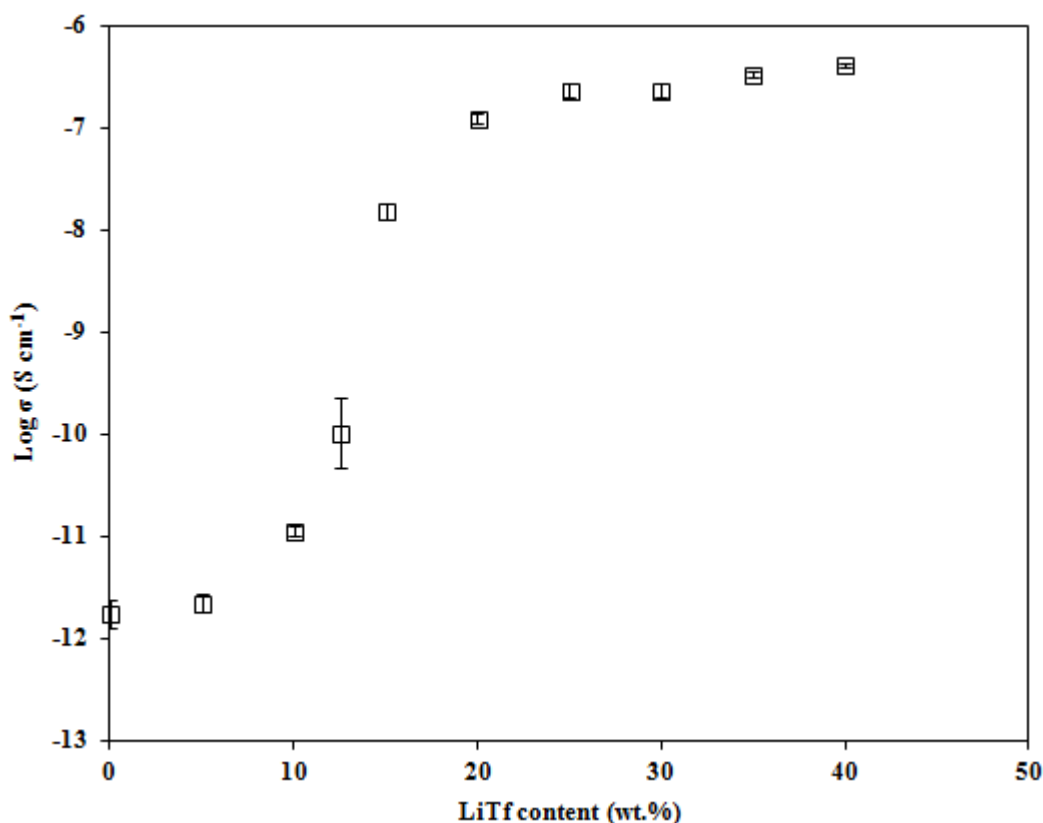


**Figure 5.2** Effect of LiTf content on the ionic conductivity at 298 K of PEMA/PVdF-HFP-based polymer electrolytes

The room temperature conductivity value achieved for S-30 is acceptable and slightly lower as compared to other polymer electrolytes containing LiTf salt, such as 85 wt. % poly(ethylene oxide), PEO-15 wt.% LiTf with  $\sigma \sim 1.3 \times 10^{-6} \text{ S cm}^{-1}$  [Karan et al., 2008] and 75 mol% poly(vinyl alcohol), PVA-25 mol% LiTf with  $\sigma = 7.06 \times 10^{-4} \text{ S cm}^{-1}$  [Malathi et al., 2010].

**Table 5.1** Ionic conductivities,  $\sigma$  of PEMA/PVdF–HFP blend films incorporated with different amounts (wt. %) of LiTf salt at 298 K

Sample	Average $R_b$ (ohm)	Average $\sigma$ (S cm <sup>-1</sup> )	Standard error (S cm <sup>-1</sup> )
S-0	$4.77 \times 10^8$	$1.82 \times 10^{-12}$	$\pm 5.94 \times 10^{-13}$
S-5	$3.81 \times 10^8$	$2.24 \times 10^{-12}$	$\pm 4.74 \times 10^{-13}$
S-10	$7.12 \times 10^7$	$1.14 \times 10^{-11}$	$\pm 1.11 \times 10^{-12}$
S-12.5	$5.35 \times 10^6$	$1.21 \times 10^{-10}$	$\pm 8.77 \times 10^{-11}$
S-15	$6.25 \times 10^4$	$1.51 \times 10^{-8}$	$\pm 2.94 \times 10^{-9}$
S-20	$6.98 \times 10^3$	$1.25 \times 10^{-7}$	$\pm 8.31 \times 10^{-8}$
S-25	$4.19 \times 10^3$	$2.28 \times 10^{-7}$	$\pm 3.44 \times 10^{-8}$
S-30	$3.35 \times 10^3$	$2.87 \times 10^{-7}$	$\pm 1.27 \times 10^{-7}$
S-35	$2.51 \times 10^3$	$3.29 \times 10^{-7}$	$\pm 2.54 \times 10^{-7}$
S-40	$2.34 \times 10^3$	$4.13 \times 10^{-7}$	$\pm 8.13 \times 10^{-7}$

### 5.2.2 Temperature Dependence Conductivity Studies

Figure 5.3 depicts the Nyquist plots of S-30 at various temperatures. It can be observed that the  $R_b$  value decreases with increasing temperature up to 353 K.

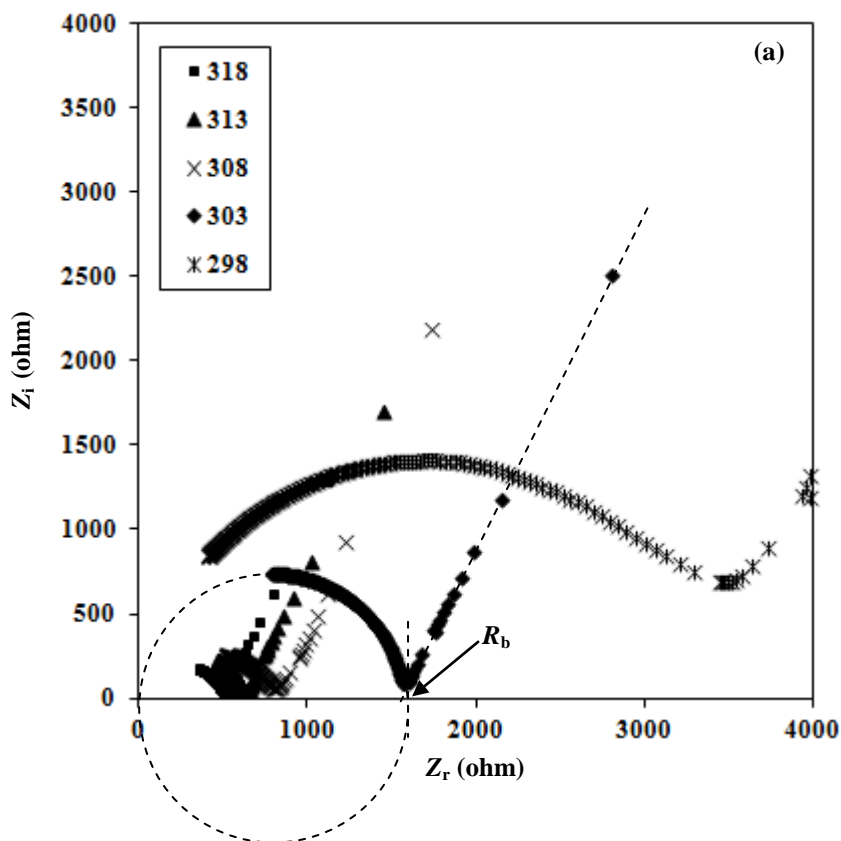


(Figure 5.3, continued)

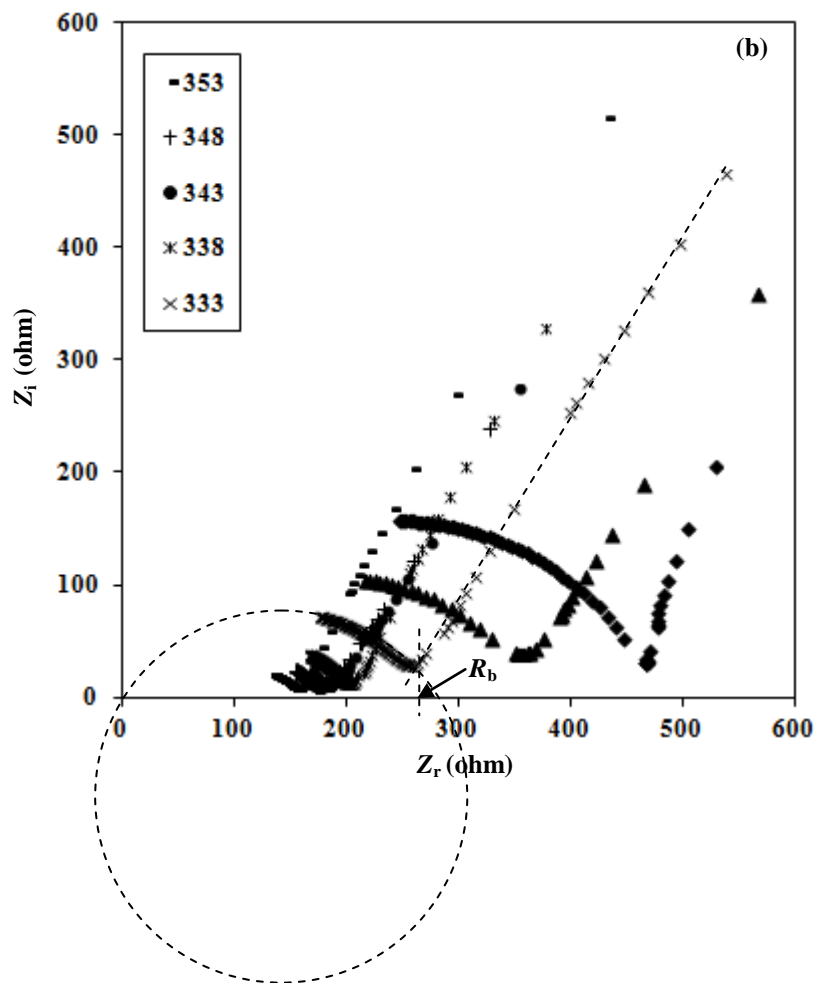


Figure 5.3 (a) and (b) Nyquist plots of S-30 at various temperatures

The decrease in  $R_b$  value of the sample can be due to the increased thermal movement of polymer segmental chains and the increased dissociation of the salt, consequently improving the ionic conductivity when temperature is increased [Raphael et al., 2010]. The temperature-dependent ionic conductivity was obtained to analyze the possible mechanism of ionic conduction in the system.  $\log \sigma$  of S-10, S-20, S-30 and S-40 were plotted against  $1000/T$  and depicted in Figure 5.4. The ionic conductivities increased with temperature from 298 K to 353 K indicating that temperature helps to dissociate the salt or increase the mobility of the ions. The plot displays Arrhenius-like behaviour whereby two linear sections with regression values,  $R^2 \sim 1$  were obtained for each sample. Using equation (2.2), two different activation energies,  $E_a$  were obtained

for the LiTf-based samples. It is inferred that the change in  $E_a$  around 308 to 313 K is attributed to a phase transition that is expected to occur around the glass transition temperature,  $T_g$  of the sample. The  $T_g$  of pure PEMA and pure PVdF-HFP is around 338 K [Smyrl and Lien, 1993] and between 240 K and 268 K [Meschede et al., 2008], respectively. For S-10, the phase transition occurs at 313 K.

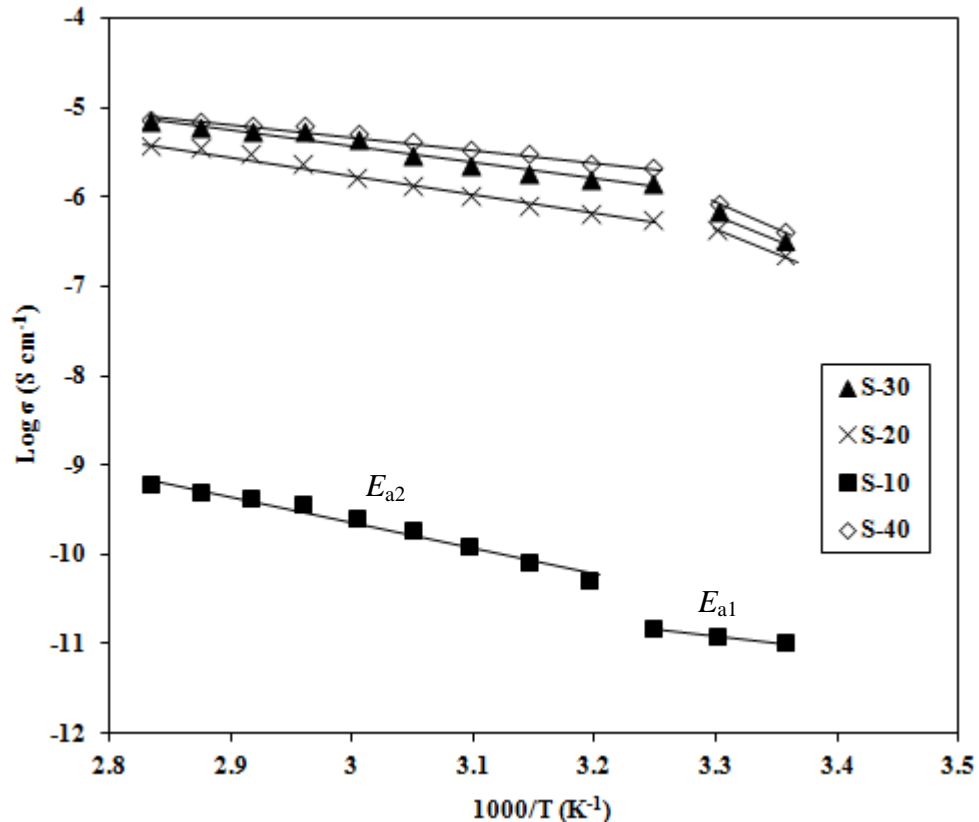


Figure 5.4 Plot of  $\log \sigma$  versus  $1000/T$  of PEMA/PVdF-HFP-LiTf polymer electrolytes

For S-20, S-30 and S-40, the phase transition occurs at lower temperature around 308 K. The activation energy before the phase transition,  $E_{a1}$  is observed to increase with LiTf content up to 40 wt.%. The activation energy after the phase transition,  $E_{a2}$  decreased with LiTf content. Table 5.2 lists the activation energies of S-10, S-20, S-30 and S-40.



**Table 5.2** Activation energy,  $E_a$  of PEMA/PVdF–HFP blend films incorporated with different amounts (wt. %) of LiTf salt

Sample	$E_{a1}$ (eV)	$E_{a2}$ (eV)
S-10	0.13	0.26
S-20	0.46	0.19
S-30	0.51	0.17
S-40	0.56	0.11

In order to investigate the effect of LiTf content on the number density ( $n$ ), mobility ( $\mu$ ) and diffusion coefficient ( $D$ ) of ions, the % area of free ions obtained from Section 4.2.3 was used to calculate  $n$  and  $\mu$  using equation (3.2) and (3.3). The data used for the calculation for  $n$ ,  $\mu$  and  $D$  for this polymer electrolyte system is shown in Appendix A. The plot of  $n$  and  $\mu$  versus LiTf content is illustrated in Figure 5.5 and their values are tabulated in Table 5.3.

**Table 5.3** Number density,  $n$ , mobility,  $\mu$  and diffusion coefficient,  $D$  of free ions for PEMA/PVdF–HFP–LiTf system

Sample	Area of free Tf ions (%)	$n$ ( $\text{cm}^{-3}$ )	$\mu$ ( $\text{cm}^2\text{V}^{-1}\text{s}^{-1}$ )	$D$ ( $\text{cm}^2\text{s}^{-1}$ )	$n\mu$ ( $\text{cm V}^{-1}\text{s}^{-1}$ )
S-10	76.1	$4.29 \times 10^{22}$	$1.66 \times 10^{-15}$	$4.26 \times 10^{-17}$	$7.12 \times 10^7$
S-20	41.9	$4.53 \times 10^{22}$	$1.72 \times 10^{-11}$	$4.43 \times 10^{-13}$	$7.80 \times 10^{11}$
S-30	65.1	$1.01 \times 10^{23}$	$1.77 \times 10^{-11}$	$4.54 \times 10^{-13}$	$1.79 \times 10^{12}$
S-40	46.8	$9.34 \times 10^{22}$	$2.76 \times 10^{-11}$	$7.08 \times 10^{-13}$	$2.58 \times 10^{12}$

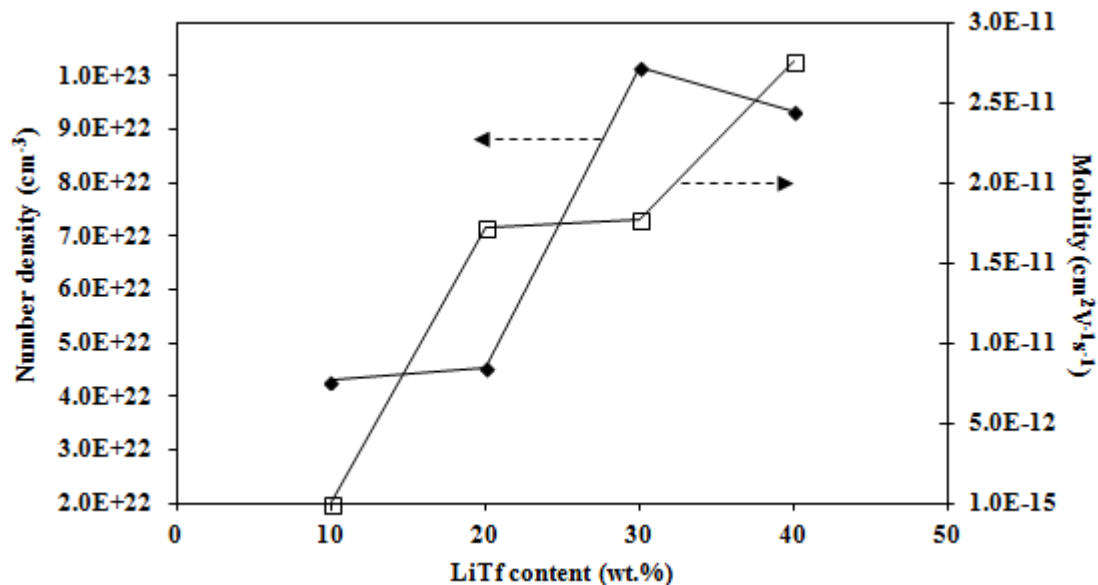


**Figure 5.5** Plot of number density and mobility in PEMA/PVdF–HFP–LiTf system

It is observed that value of  $n$  increased with increasing LiTf from S-0 to S-30, after which a decrease was observed in S-40. The  $\mu$  increased up to 40 wt.% LiTf.

### 5.3 Plasticized PEMA/PVdF-HFP-LiTf Polymer Electrolyte Systems

#### 5.3.1 PEMA/PVdF-HFP-LiTf-EC System

##### 5.3.1.1 Composition Dependence Conductivity Studies

For PEMA/PVdF-HFP-LiTf-EC system, the  $\text{Li}^+$  and  $\text{Tf}^-$  ions from LiTf salt are the conducting ions. The Nyquist plots of EC-containing polymer electrolytes are shown in Figure 5.6.

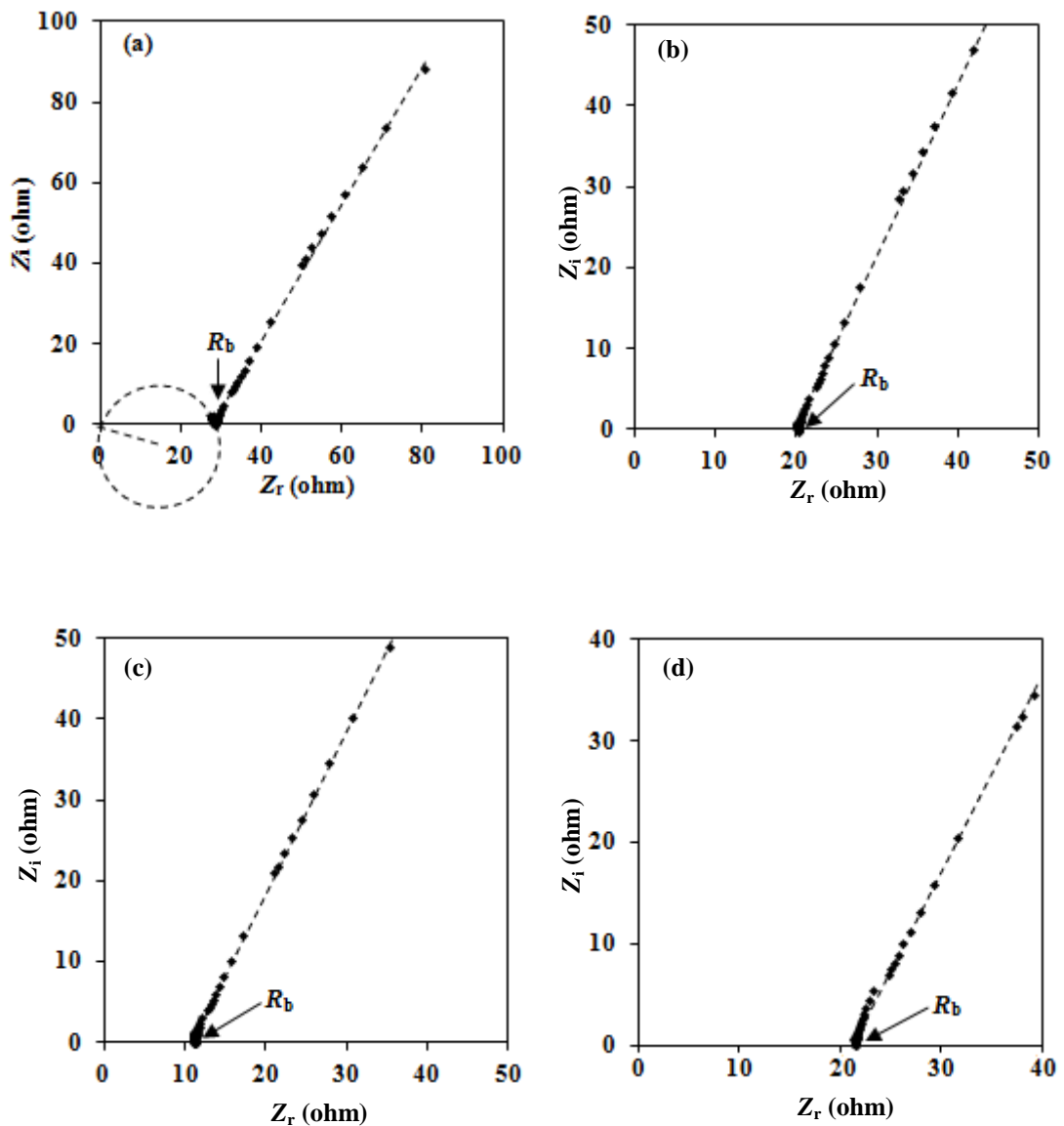


(Figure 5.6, continued)

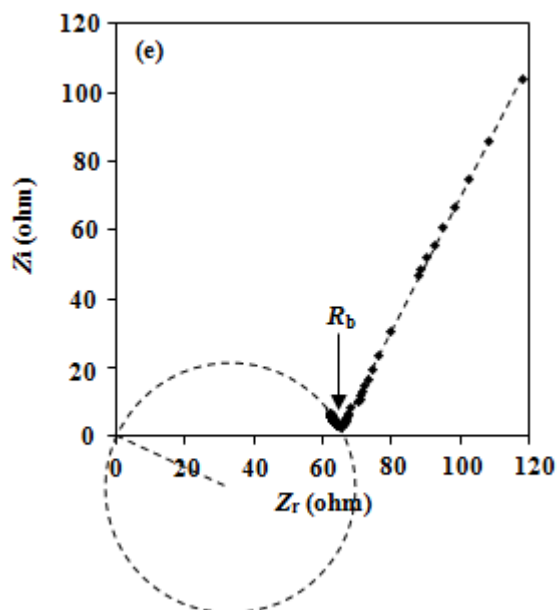


Figure 5.6 Nyquist plots of (a) EC-2, (b) EC-4, (c) EC-6, (d) EC-8 and (e) EC-10 films

The Nyquist plots for EC-2 and EC-10 samples show a spike at low frequency and part of a semicircle at higher frequencies while that of other samples only show a spike at low frequency. The absence of a semicircle at high frequency suggests the absence of capacitive nature and that only diffusion process occurs [Baskaram et al., 2004]. Hence, current carriers are ions and the total conductivity is mainly due to ionic conduction. The bulk resistance,  $R_b$  was obtained from the intercept of the low frequency spike with the real axis. The  $R_b$  value decreased upon incorporation of EC until 6 wt.%, above which the  $R_b$  gradually increased up to 10 wt.% EC.

The EC composition dependence of the room temperature ionic conductivity of PEMA/PVdF-HFP-LiTf-EC system is displayed in Figure 5.7. Upon addition of EC, the ionic conductivity increased to reach its maximum at 6 wt.% EC with  $\sigma = 1.05 \times 10^{-4} \text{ S cm}^{-1}$  which is three orders of magnitude higher than EC-0 sample. Above 6 wt.% EC, the ionic conductivity dropped with increasing EC content. Table 5.4 lists the ionic conductivity values of PEMA/PVdF-HFP-LiTf-EC polymer electrolyte system.

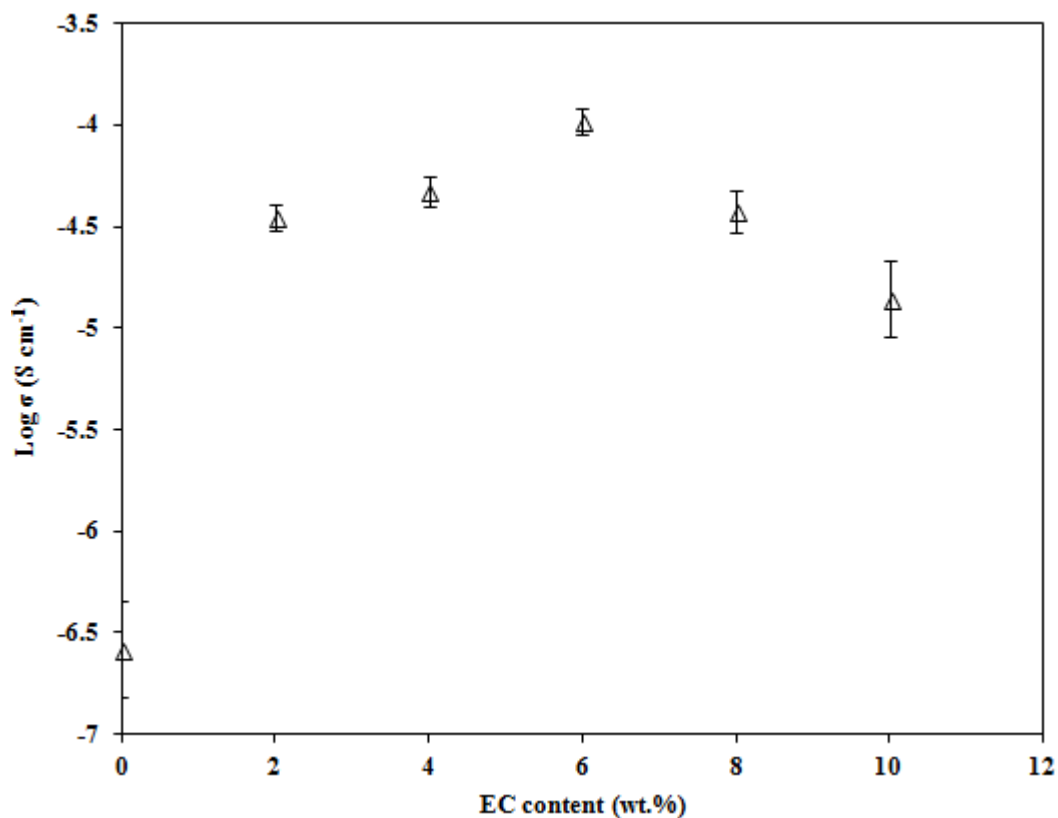
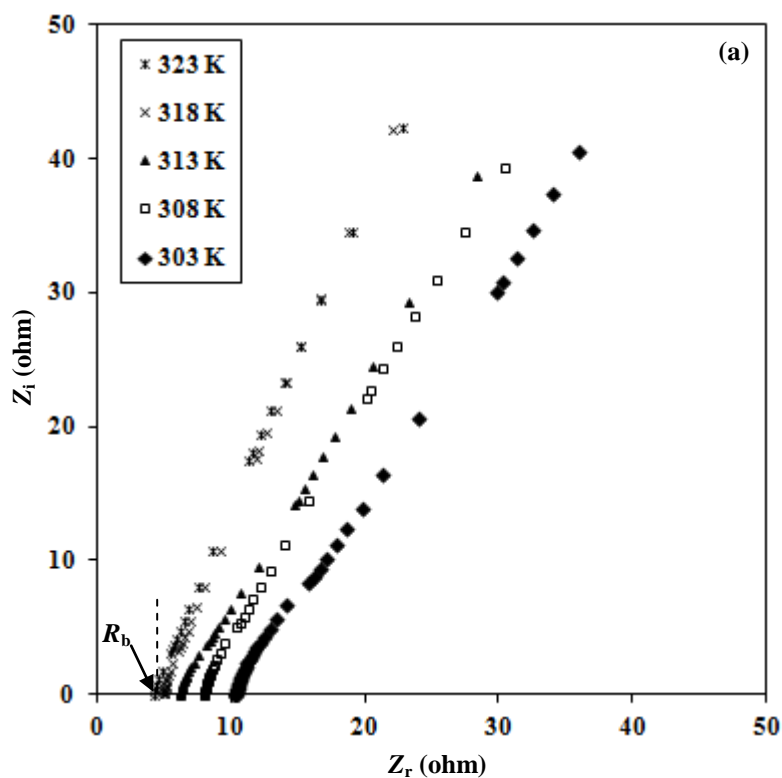


Figure 5.7 Effect of EC content on the ionic conductivity at 298 K of PEMA/PVdF–HFP–LiTf based polymer electrolytes

### 5.3.1.2 Temperature Dependence Conductivity Studies

The Nyquist plots of EC–6 at various temperatures are depicted in Figure 5.8.



(Figure 5.8, continued)

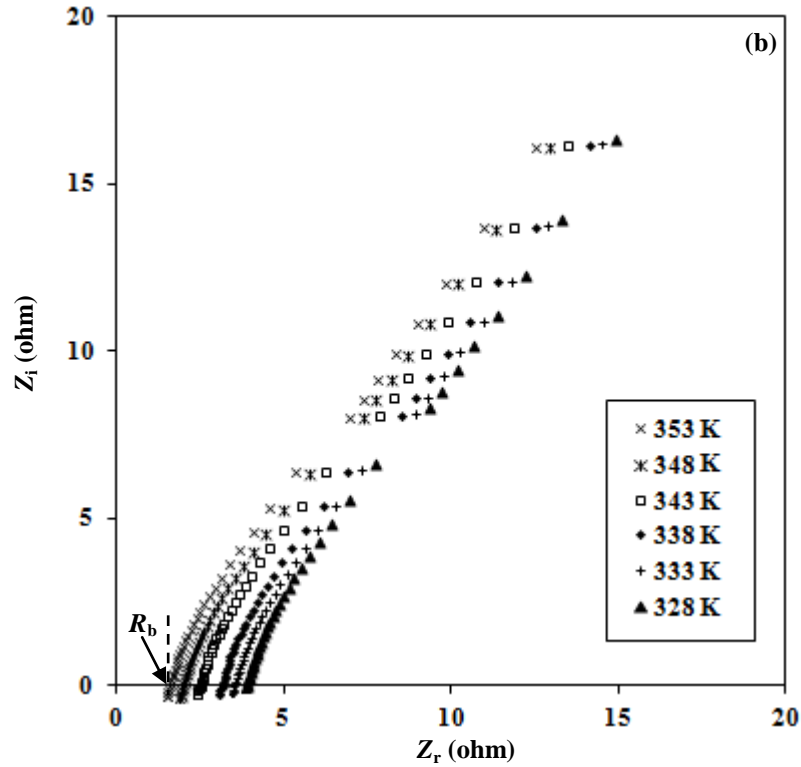


Figure 5.8 (a) and (b) Nyquist plots of EC-6 at various temperatures

It can be observed that the  $R_b$  value decreased with increasing temperature. The temperature dependent ionic conductivities of EC-incorporated system are shown in Figure 5.9. Curvature plots of  $\log \sigma$  versus  $1000/T$  were obtained for all EC-containing samples which indicates that the ionic conduction follows the Vogel Tamman Fulcher (VTF) model. According to VTF model, the ionic conduction is assisted by polymer segmental motion which helps ions to be transported from one coordination site to another in a polymer electrolyte [Uma et al., 2003]. The values of the ideal glass transition temperature,  $T_0$  were determined by trial and error using equation (2.3) in order to obtain the highest  $R^2$  value nearest to unity for each plot in Figure 5.10. The  $R^2$  value obtained from the plot of  $\log(\sigma T^{1/2})$  versus  $1000/(T-T_0)$  for all EC-added samples was found to be 0.99. The  $T_0$  values used are listed in Table 5.3 and were found to increase in the order of EC-6 < EC-4 < EC-8 < EC-2 < EC-10.

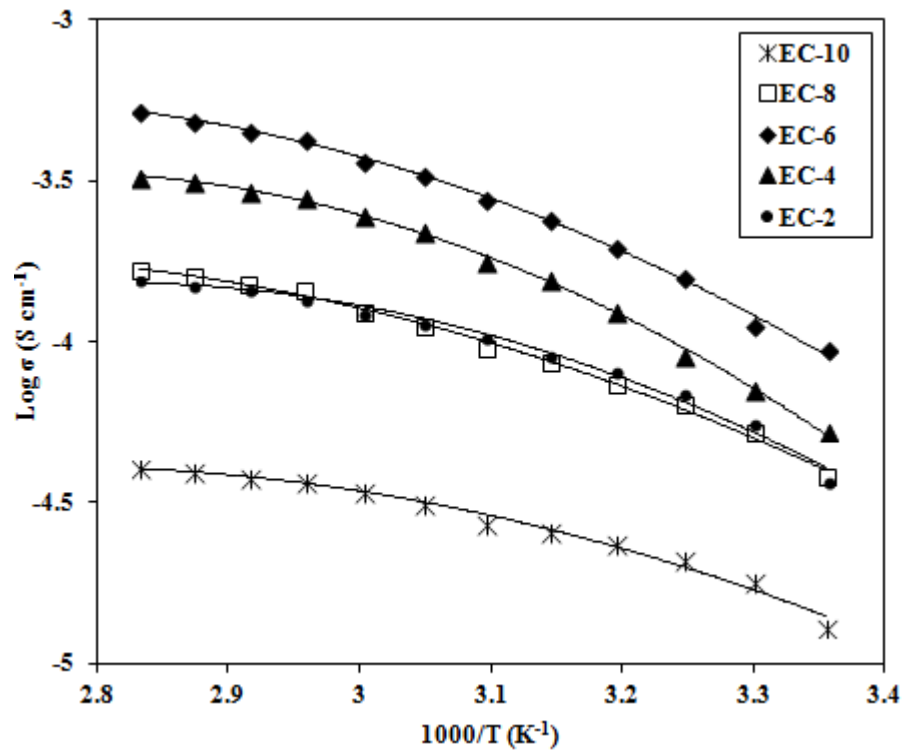


Figure 5.9 Plot of  $\log \sigma$  versus  $1000/T$  of PEMA/PVdF-HFP-LiTf-EC polymer electrolytes

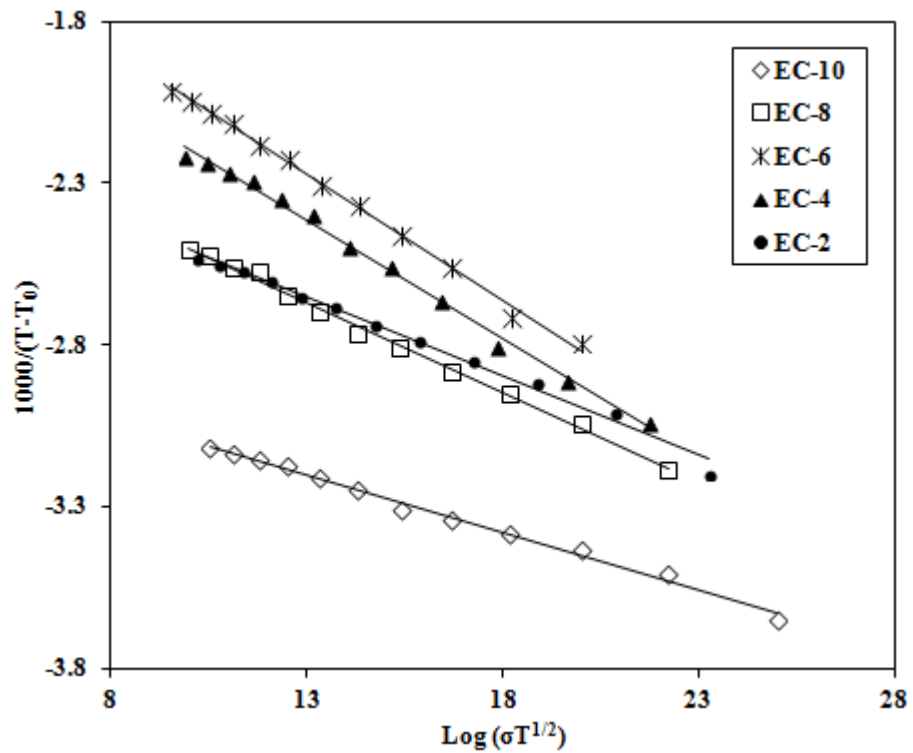


Figure 5.10 Plot of  $\log(\sigma T^{1/2})$  versus  $1000/(T-T_0)$  of PEMA/PVdF-HFP-LiTf-EC polymer electrolytes

Table 5.4 Ionic conductivities,  $\sigma$  of PEMA/PVdF–HFP–LiTf blend films incorporated with different EC contents at 298 K

Sample	Average $R_b$ (ohm)	Average $\sigma$ (S cm <sup>-1</sup> )	Standard error (S cm <sup>-1</sup> )	$R^2$	$T_0$ (K)
EC-2	28.6	$3.53 \times 10^{-5}$	$\pm 4.95 \times 10^{-6}$	0.9912	255
EC-4	20.5	$4.77 \times 10^{-5}$	$\pm 7.78 \times 10^{-6}$	0.9949	252
EC-6	11.6	$1.05 \times 10^{-4}$	$\pm 1.53 \times 10^{-5}$	0.9964	244
EC-8	21.4	$3.80 \times 10^{-5}$	$\pm 8.77 \times 10^{-6}$	0.9960	253
EC-10	64.5	$1.20 \times 10^{-5}$	$\pm 5.16 \times 10^{-6}$	0.9925	258

The effect of EC content on the values of  $n$  and  $\mu$  are illustrated in Figure 5.11 and the results are tabulated in Table 5.5. The data used for the calculation is shown in Appendix B. The value of  $n$  was observed to decrease as EC content was increased up to 10 wt.%. The ion mobility,  $\mu$  was shown to increase up to a maximum at 6 wt.% EC before decreasing above that content. The ionic conductivity trend is governed by the mobility.

Table 5.5 Number density,  $n$ , mobility,  $\mu$  and diffusion coefficient,  $D$  of free ions for PEMA/PVdF–HFP–LiTf–EC system

Sample	Area of free ions (%)	$n$ (cm <sup>-3</sup> )	$\mu$ (cm <sup>2</sup> V <sup>-1</sup> s <sup>-1</sup> )	$D$ (cm <sup>2</sup> s <sup>-1</sup> )	$n\mu$ (cmV <sup>-1</sup> s <sup>-1</sup> )
EC-2	51.1	$7.81 \times 10^{22}$	$2.82 \times 10^{-9}$	$7.24 \times 10^{-11}$	$2.20 \times 10^{14}$
EC-4	38.4	$5.76 \times 10^{22}$	$5.17 \times 10^{-9}$	$1.33 \times 10^{-10}$	$2.98 \times 10^{14}$
EC-6	26.5	$3.91 \times 10^{22}$	$1.68 \times 10^{-8}$	$4.31 \times 10^{-10}$	$6.55 \times 10^{14}$
EC-8	33.8	$4.88 \times 10^{22}$	$4.86 \times 10^{-9}$	$1.25 \times 10^{-10}$	$2.37 \times 10^{14}$
EC-10	42.1	$5.96 \times 10^{22}$	$1.26 \times 10^{-9}$	$3.23 \times 10^{-11}$	$7.49 \times 10^{13}$

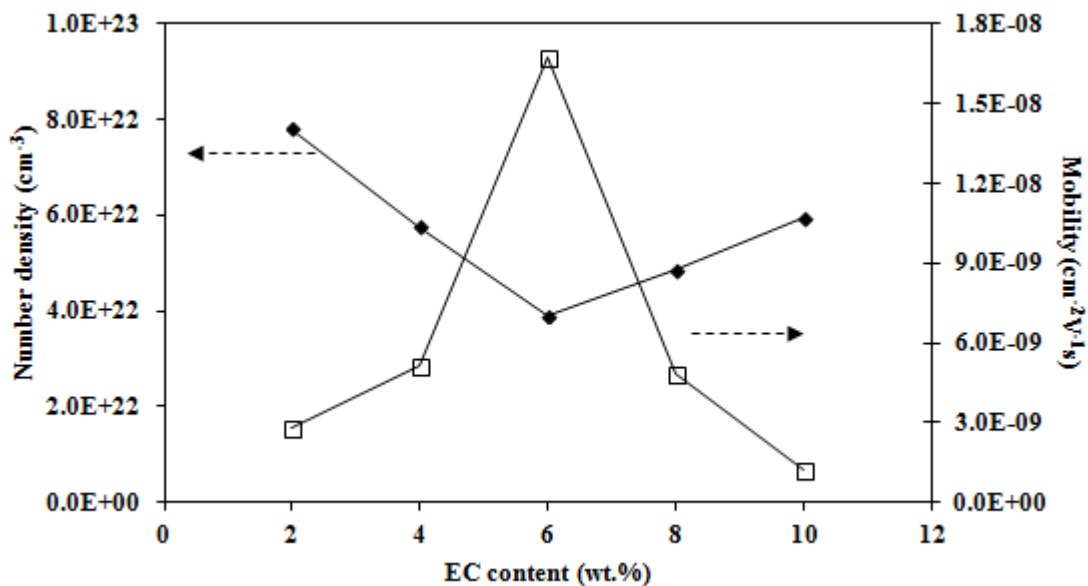
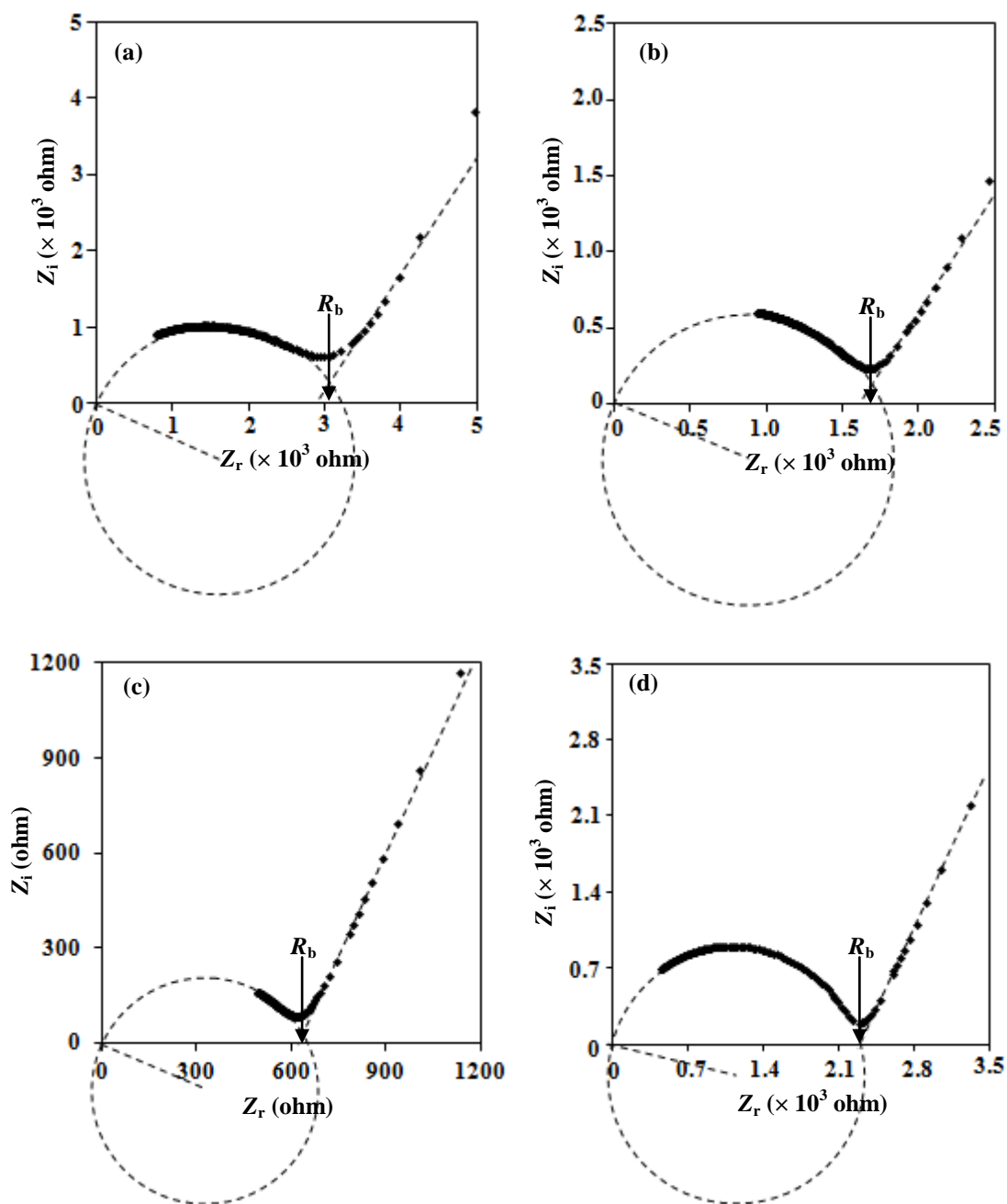


Figure 5.11 Plot of number density and mobility in PEMA/PVdF–HFP–LiTf–EC system  
 5.3.2 PEMA/PVdF–HFP–LiTf–PC System

### 5.3.2.1 Composition Dependence Conductivity Studies

For this system,  $\text{Li}^+$  and  $\text{Tf}^-$  ions from LiTf salt are the conducting ions. The Nyquist plots of PC-containing polymer electrolytes are shown in Figure 5.12.





(Figure 5.12, continued)

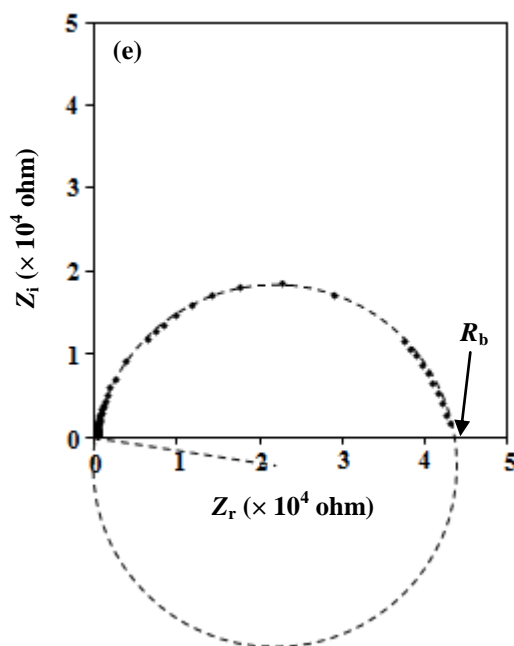


Figure 5.12 Nyquist plots of (a) PC-2, (b) PC-4, (c) PC-6, (d) PC-8 and (e) PC-10 films

An incomplete semicircle at higher frequencies and a spike at lower frequencies were observed in PC-2, PC-4, PC-6 and PC-8 samples, Figure 5.12 (a) to (d). A depressed semicircle with the absence of spike was observed in PC-10 sample, Figure 5.12 (e). The  $R_b$  value decreased continuously upon addition of PC up to 6 wt.%. Above that content, the  $R_b$  value increased gradually. The plot of ionic conductivity versus PC content is depicted in Figure 5.13.

The ionic conductivity was observed to increase with addition of PC up to 6 wt.% at  $1.46 \times 10^{-6} \text{ S cm}^{-1}$  which is about one order of magnitude higher than PC-0 sample. As more PC was added into the 70 wt.% [PEMA/PVdF-HFP]-30 wt.% LiTf composition, the ionic conductivity dropped. The ionic conductivity values of PC-based polymer electrolyte system are listed in Table 5.6.

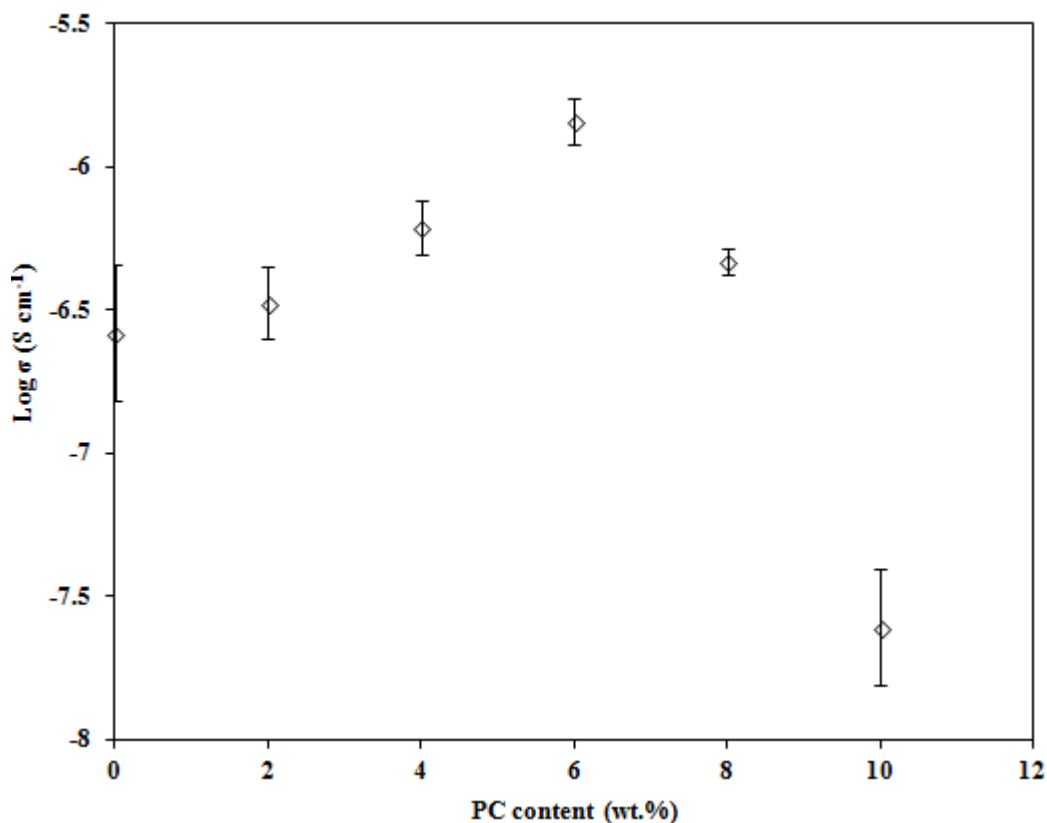


Figure 5.13 Effect of PC content on the ionic conductivity at 298 K of PEMA/PVdF–HFP–LiTf based polymer electrolytes

### 5.3.2.2 Temperature Dependence Conductivity Studies

Figure 5.14 shows the Nyquist plots of PC–6 sample at various temperatures. The  $R_b$  value was observed to decrease with increasing temperature up to 353 K. Figure 5.15 illustrates the plots of  $\log \sigma$  versus  $1000/T$  for PC–based system. The curved  $\log \sigma$  versus  $1000/T$  plots in Figure 5.15 indicate that the ionic conduction obeys the VTF equation. Following that,  $\log (\sigma T^{1/2})$  versus  $1000/(T-T_0)$  were plotted as shown in Figure 5.16 by substituting the  $T_0$  value obtained by trial and error into equation (2.3). The  $R^2$  values obtained lie between 0.97 and 0.99. The  $T_0$  values obtained follow the conductivity trend and goes in the increasing order of PC–6 < PC–4 < PC–8 < PC–2 < PC–10. The  $T_0$  and  $R^2$  values of PC–based system are listed in Table 5.6.

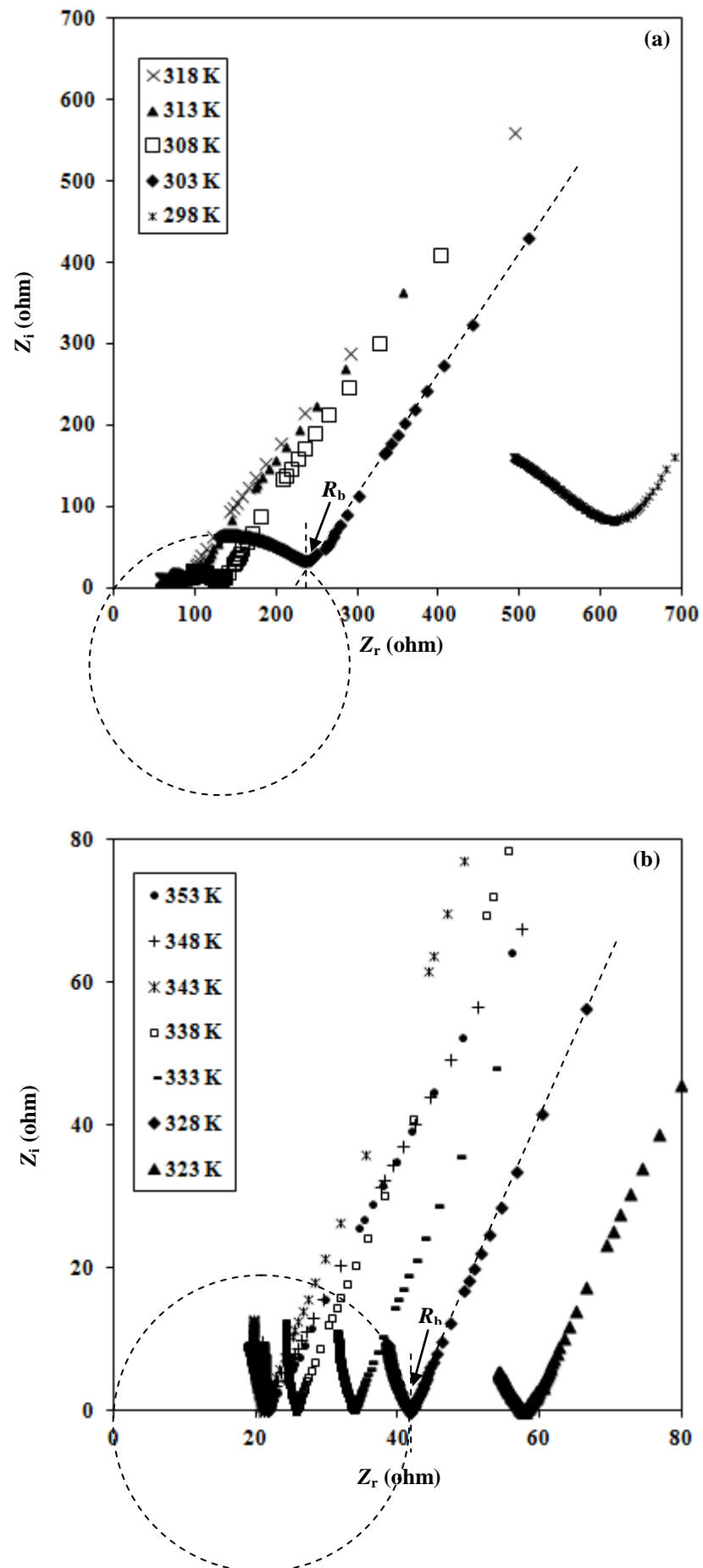


Figure 5.14 (a) and (b) Nyquist plots of PC-6 at various temperatures

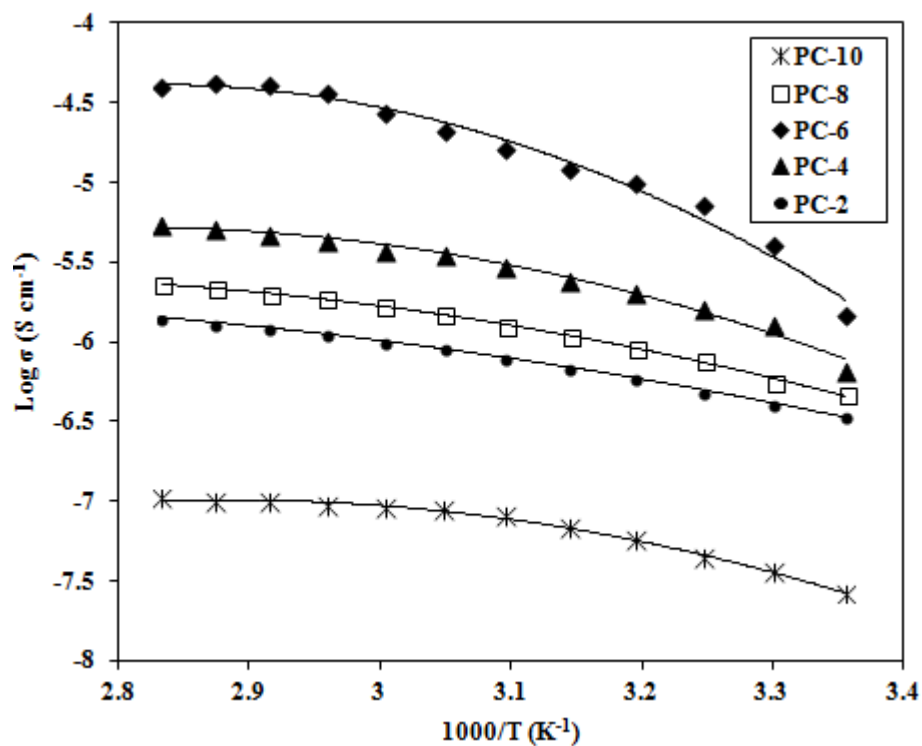


Figure 5.15 Plot of  $\log \sigma$  versus  $1000/T$  of PEMA/PVdF-HFP-LiTf-PC polymer electrolytes

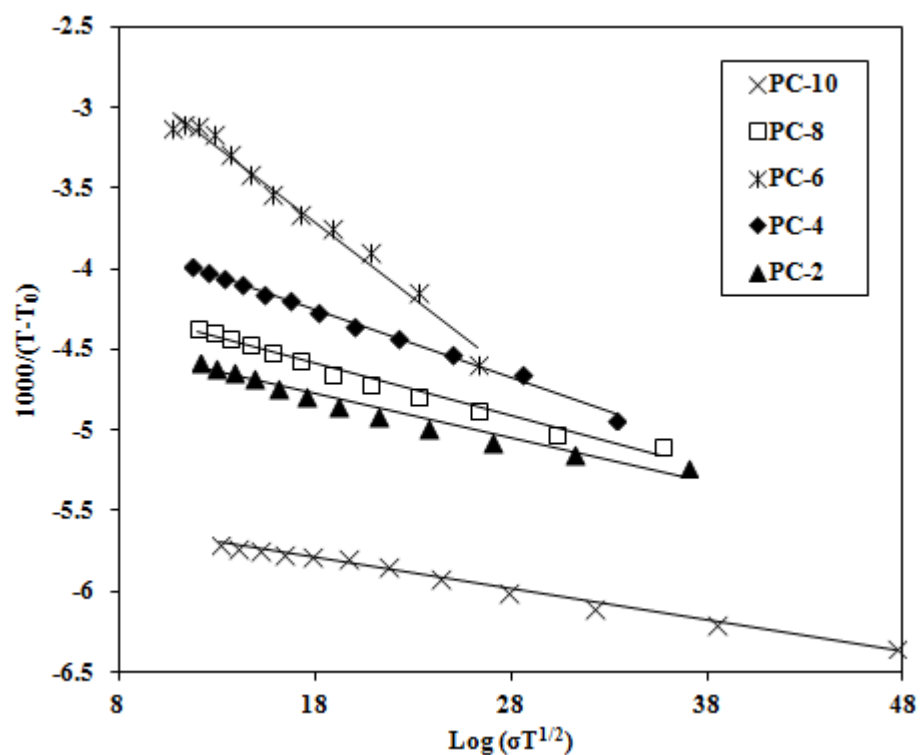
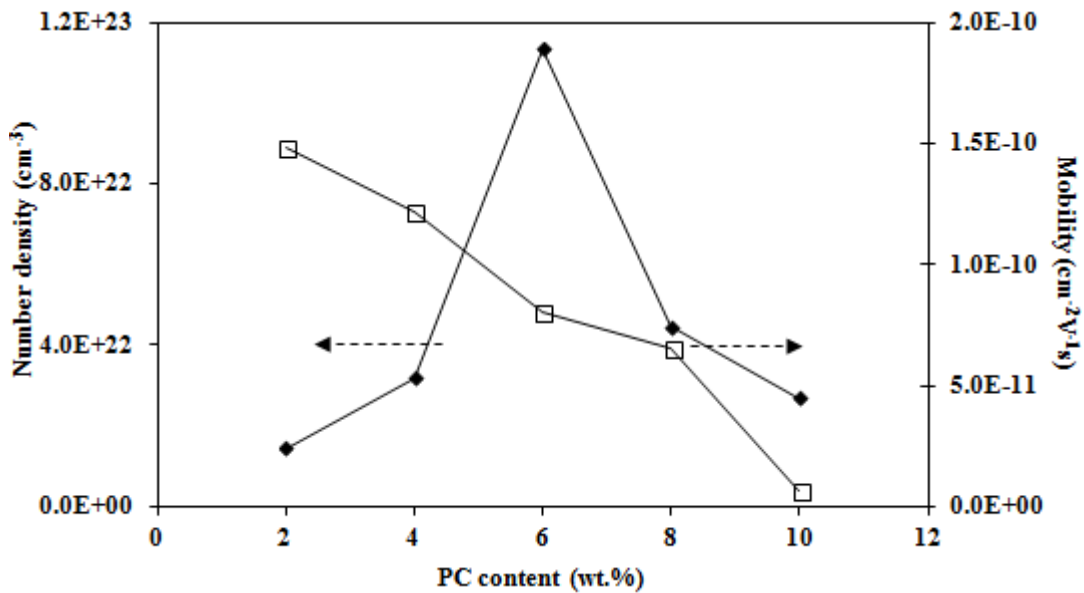


Figure 5.16 Plot of  $\log(\sigma T^{1/2})$  versus  $1000/(T-T_0)$  of PEMA/PVdF-HFP-LiTf-PC polymer electrolytes

**Table 5.6** Ionic conductivities,  $\sigma$  of PEMA/PVdF–HFP–LiTf blend films incorporated with different PC contents at 298 K

Sample	Average $R_b$ (ohm)	Average $\sigma$ (S cm <sup>-1</sup> )	Standard error (S cm <sup>-1</sup> )	$R^2$	$T_0$ (K)
PC-2	3070	$3.43 \times 10^{-7}$	$\pm 9.76 \times 10^{-8}$	0.9705	271
PC-4	1686	$6.23 \times 10^{-7}$	$\pm 1.34 \times 10^{-7}$	0.9950	268
PC-6	625	$1.46 \times 10^{-6}$	$\pm 2.76 \times 10^{-7}$	0.9841	264
PC-8	2280	$4.70 \times 10^{-7}$	$\pm 5.24 \times 10^{-8}$	0.9835	270
PC-10	43700	$2.65 \times 10^{-8}$	$\pm 1.19 \times 10^{-8}$	0.9903	277

Figure 5.17 depicts the effect of PC on the values of  $n$  and  $\mu$ . The data used for the calculation is shown in Appendix C and the results are listed in Table 5.7. The  $n$  increased up to 6 wt.% before decreasing at higher PC content. On the other hand, the  $\mu$  was observed to decrease with increasing PC content, which correlates to the ionic conductivity trend.



**Figure 5.17** Plot of number density and mobility in PEMA/PVdF–HFP–LiTf–PC system

**Table 5.7** Number density,  $n$ , mobility,  $\mu$  and diffusion coefficient,  $D$  of free ions for PEMA/PVdF–HFP–LiTf–PC system

Sample	Area of free ions (%)	$n$ (cm <sup>-3</sup> )	$\mu$ (cm <sup>2</sup> V <sup>-1</sup> s <sup>-1</sup> )	$D$ (cm <sup>2</sup> s <sup>-1</sup> )	$n\mu$ (cm V <sup>-1</sup> s <sup>-1</sup> )
PC-2	9.4	$1.44 \times 10^{22}$	$1.48 \times 10^{-10}$	$3.81 \times 10^{-12}$	$2.14 \times 10^{12}$
PC-4	21.2	$3.20 \times 10^{22}$	$1.22 \times 10^{-10}$	$3.12 \times 10^{-12}$	$3.89 \times 10^{12}$
PC-6	76.6	$1.13 \times 10^{23}$	$8.04 \times 10^{-11}$	$2.06 \times 10^{-12}$	$9.11 \times 10^{12}$
PC-8	30.7	$4.47 \times 10^{22}$	$6.57 \times 10^{-11}$	$1.69 \times 10^{-12}$	$2.93 \times 10^{12}$
PC-10	18.9	$2.70 \times 10^{22}$	$6.12 \times 10^{-12}$	$1.53 \times 10^{-13}$	$1.65 \times 10^{11}$

## 5.4 Ionic Liquid Based PEMA/PVdF–HFP Polymer Electrolyte Systems

### 5.4.1 PEMA/PVdF–HFP–LiTf–BMII System

#### 5.4.1.1 Composition Dependence Conductivity Studies

For this system, the ionic conducting species are  $\text{Li}^+$  and  $\text{Tf}^-$  ions which come from LiTf salt, as well as  $\text{BMI}^+$  and  $\Gamma^-$  ions from BMII ionic liquid. The Nyquist plots for BMII-added polymer electrolyte system are shown in Figure 5.18. All samples except BI–12.5 and BI–15 (Figure 5.18 (c) and (d)) exhibit a semicircle at higher frequencies with a spike at lower frequencies.

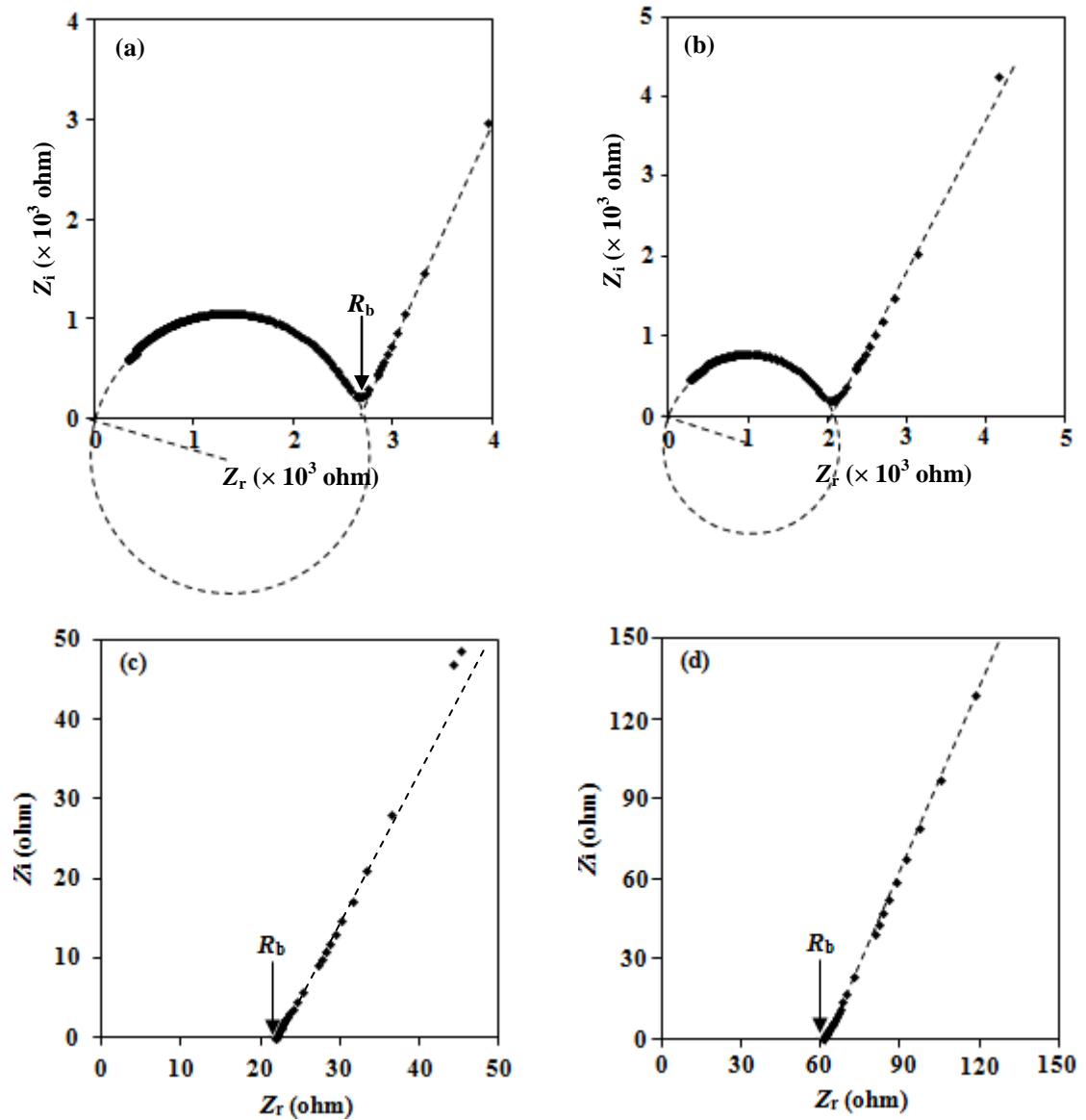


(Figure 5.18, continued)

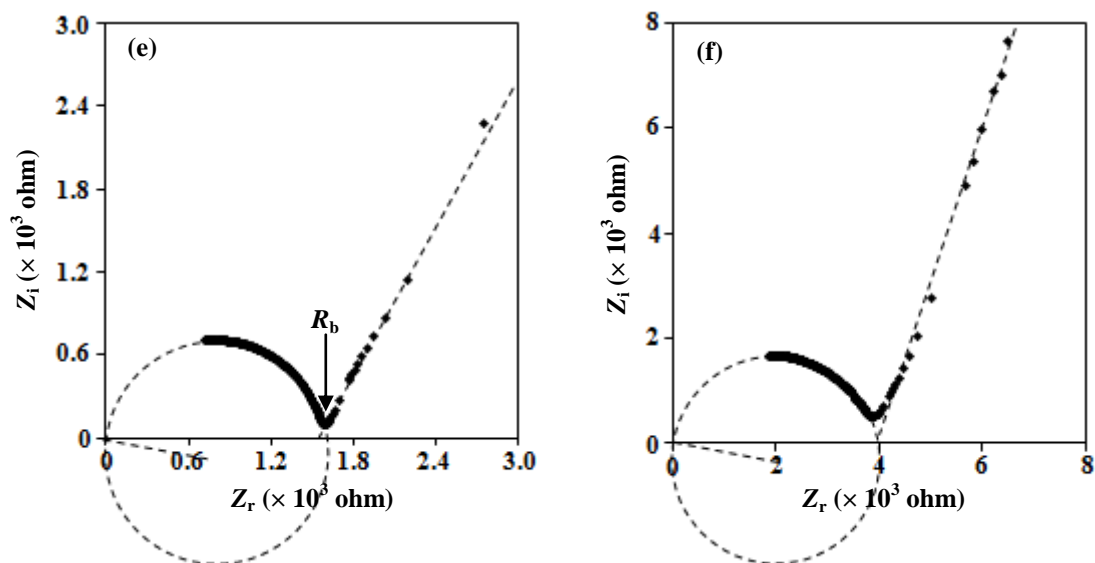


Figure 5.18 Nyquist plots of (a) BI-5, (b) BI-10, (c) BI-12.5, (d) BI-15, (e) BI-17.5 and (f) BI-20 films

The  $R_b$  value was observed to decrease from the order of thousands ohm in BI-5 to 76.1 ohm in BI-12.5 sample. Beyond 12.5 wt.% BMII,  $R_b$  increased. The room temperature conductivity of BMII-based system is plotted against BMII content in Figure 5.19.

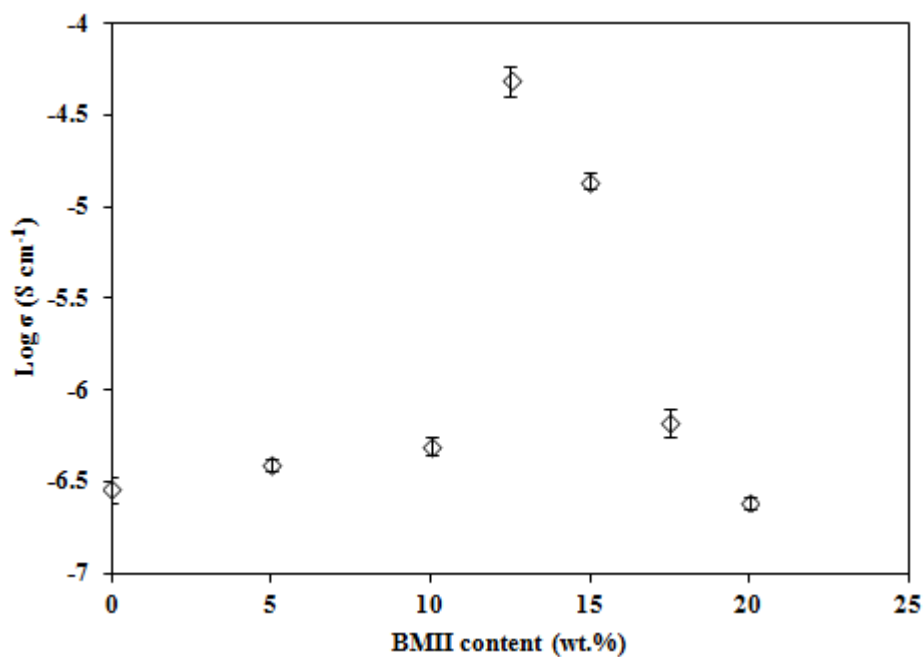
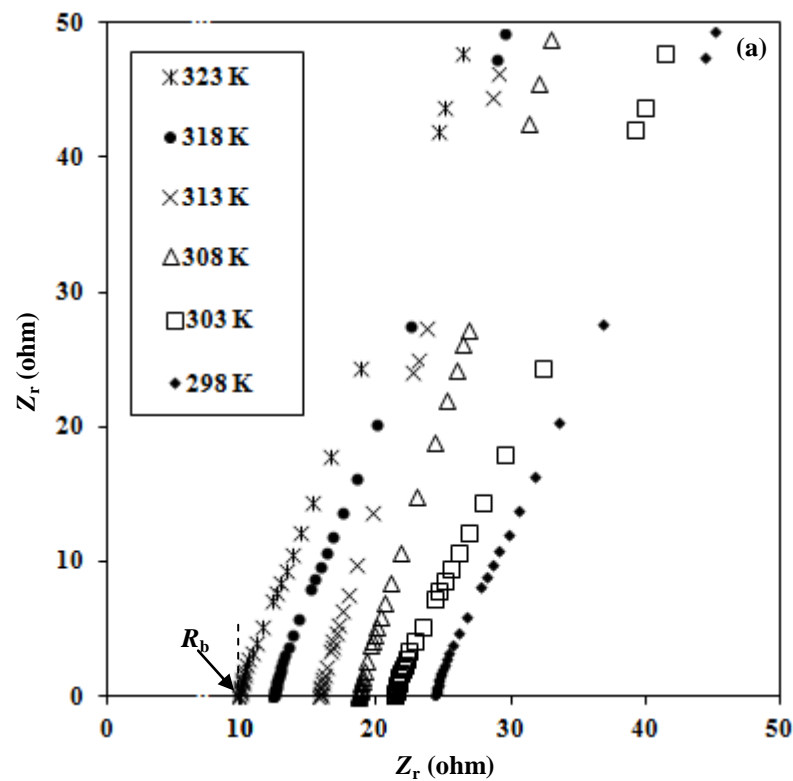


Figure 5.19 Effect of BMII content on the ionic conductivity at 298 K of PEMA/PVdF-HFP-LiTf based polymer electrolytes

The ionic conductivity was found to increase upon addition of BMII from the order of  $10^{-7}$  S  $\text{cm}^{-1}$  in BI-0 sample to the highest conductivity of  $4.86 \times 10^{-5}$  S  $\text{cm}^{-1}$  in BI-12.5 sample. The ionic conductivity decreased above 12.5 wt.% BMII. Table 5.8 lists the ionic conductivity values of BMII-added samples.

#### 5.4.1.2 Temperature Dependence Conductivity Studies

In order to study the ion conduction mechanism of BMII-based system, the Nyquist plots of BI-12.5 film at various temperatures between ambient and 353 K are shown in Figure 5.20. The  $R_b$  decreased from 21.5 ohm at 298 K with increasing temperature to 3.45 ohm at 353 K. This shows that ionic conductivity increased with increasing temperature up to 353 K. The conductivity of BMII-containing samples were plotted against temperature as depicted in Figure 5.21.





(Figure 5.20, continued)

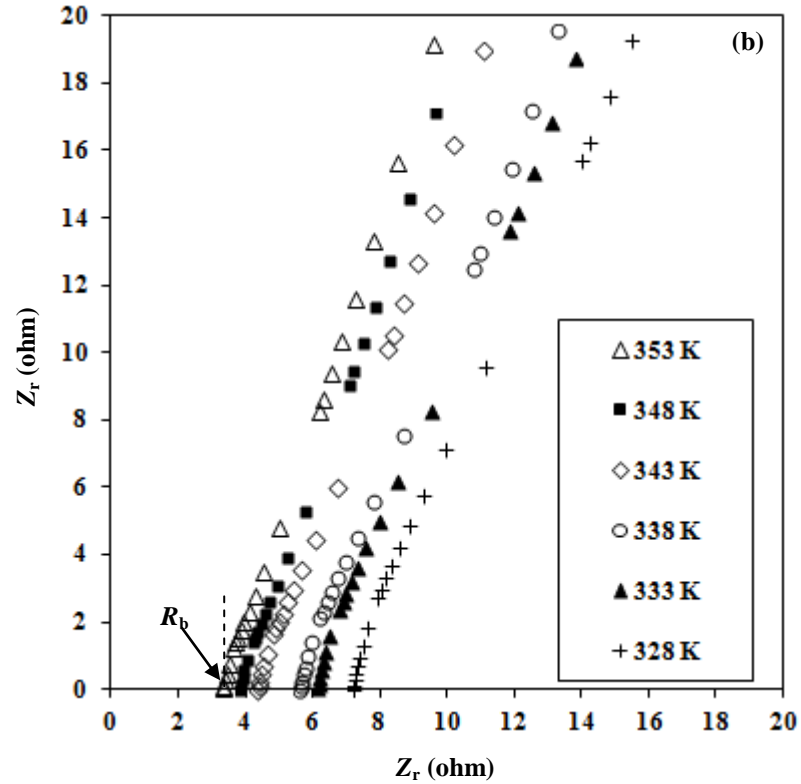


Figure 5.20 (a) and (b) Nyquist plots of BI-12.5 at various temperatures

The conductivity increased linearly with temperature although two linear sections were observed. A change in slope of each plot was observed to occur at around 308 to 313 K indicating that phase transition occurred at that temperature range. This suggests that two different  $E_a$  values exist for each plot.  $E_{a1}$  which occurs below at 313 K lies between 0.05 eV and 0.14 eV while  $E_{a2}$  was found between 0.16 eV and 0.28 eV. Both  $E_{a1}$  and  $E_{a2}$  were observed to increase in the order of BI-12.5 < BI-15 < BI-17.5 < BI-10 < BI-5 < BI-20. The activation energies of BMII-added samples are tabulated in Table 5.8.

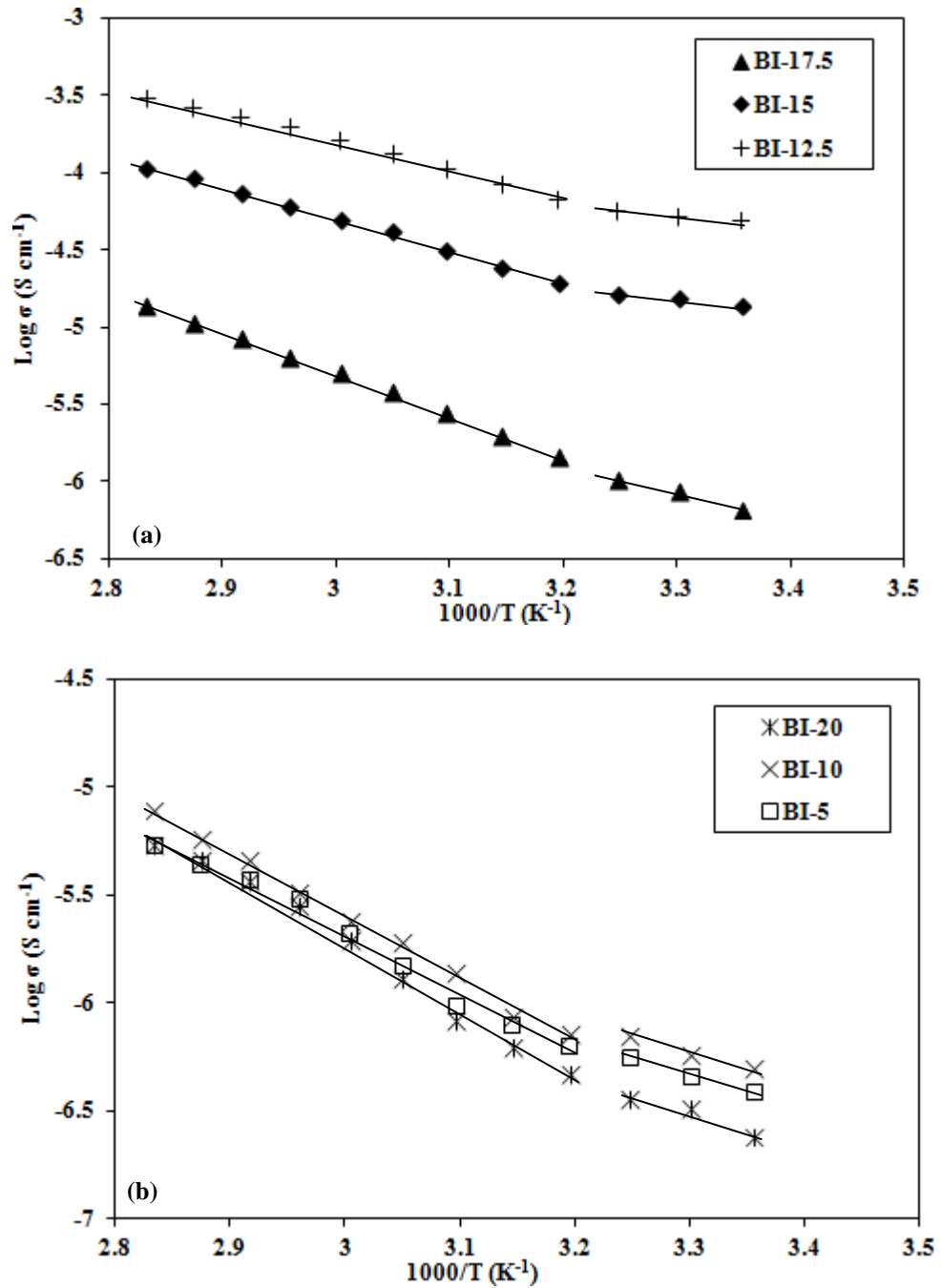


Figure 5.21 (a) and (b) Plot of  $\log \sigma$  versus  $1000/T$  of PEMA/PVdF-HFP-LiTf-BMII polymer electrolytes

Table 5.8 Ionic conductivities,  $\sigma$  and activation energies,  $E_a$  of PEMA/PVdF-HFP-LiTf blend films incorporated with different BMII contents at 298 K

Sample	Average $R_b$ (ohm)	Average $\sigma$ ( $S\ cm^{-1}$ )	Standard error ( $S\ cm^{-1}$ )	$E_{a1}$ (eV)	$E_{a2}$ (eV)
BI-5	2700	$3.88 \times 10^{-7}$	$\pm 1.05 \times 10^{-9}$	0.13	0.27
BI-10	2070	$4.94 \times 10^{-7}$	$\pm 4.62 \times 10^{-9}$	0.12	0.26
BI-12.5	21.9	$4.86 \times 10^{-5}$	$\pm 9.75 \times 10^{-6}$	0.05	0.16
BI-15	62.0	$1.38 \times 10^{-5}$	$\pm 6.54 \times 10^{-6}$	0.06	0.18
BI-17.5	1577	$6.63 \times 10^{-7}$	$\pm 8.92 \times 10^{-8}$	0.10	0.24
BI-20	3907	$2.43 \times 10^{-7}$	$\pm 3.32 \times 10^{-8}$	0.14	0.28

For BMII-added system, the total values of  $n$  were calculated by summing the number densities of  $\text{Li}^+$ ,  $\text{Tf}^-$ ,  $\text{BMI}^+$  and  $\text{I}^+$  ions. It is assumed that the ions in ionic liquids, which in this case is BMII, are totally ionized as reported in literature [1]. The values of  $\mu$  were then calculated using the total  $n$  values obtained. The data used for the calculation of  $n$ ,  $\mu$  and  $D$  for this system is shown in Appendix D. The values of  $n$  and  $\mu$  were plotted against BMII content as depicted in Figure 5.22 and the results are tabulated in Table 5.9. The  $n$  increased upon addition of 5 wt.% BMII to reach its maximum at 12.5 wt.% after which it decreased with increasing BMII content. On the other hand, the  $\mu$  only increased dramatically from 10 wt.% BMII and was highest at 12.5 wt.%. Above 12.5 wt.%,  $\mu$  decreased.

Table 5.9 Number density,  $n$ , mobility,  $\mu$  and diffusion coefficient,  $D$  of free ions for PEMA/PVdF-HFP-LiTf-BMII system

Sample	Area of free ions (%)	$n$ ( $\text{cm}^{-3}$ )	$\mu$ ( $\text{cm}^2\text{V}^{-1}\text{s}^{-1}$ )	$D$ ( $\text{cm}^2\text{s}^{-1}$ )	$n\mu$ ( $\text{cmV}^{-1}\text{s}^{-1}$ )
BI-5	9.6	$2.94 \times 10^{22}$	$8.22 \times 10^{-11}$	$1.93 \times 10^{-12}$	$2.42 \times 10^{12}$
BI-10	68.9	$1.27 \times 10^{23}$	$2.43 \times 10^{-11}$	$5.71 \times 10^{-13}$	$3.08 \times 10^{12}$
BI-12.5	92.3	$1.64 \times 10^{23}$	$1.85 \times 10^{-9}$	$4.36 \times 10^{-11}$	$3.03 \times 10^{14}$
BI-15	18.8	$7.05 \times 10^{22}$	$1.22 \times 10^{-9}$	$2.87 \times 10^{-11}$	$8.61 \times 10^{13}$
BI-17.5	11.5	$6.80 \times 10^{22}$	$6.09 \times 10^{-11}$	$1.43 \times 10^{-12}$	$4.14 \times 10^{12}$
BI-20	5.4	$6.76 \times 10^{22}$	$2.24 \times 10^{-11}$	$5.28 \times 10^{-13}$	$1.52 \times 10^{12}$

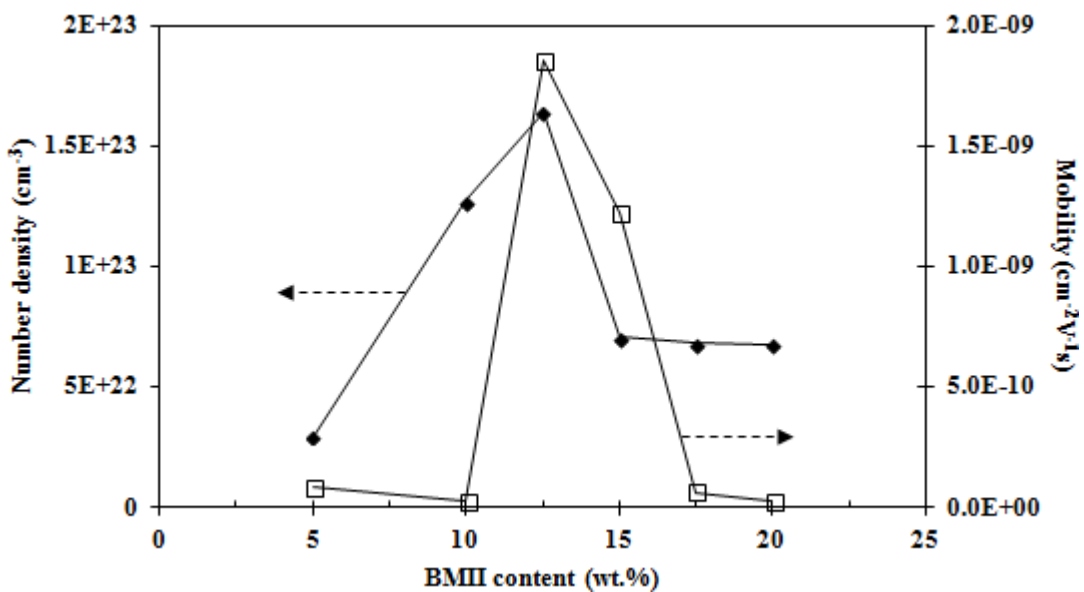
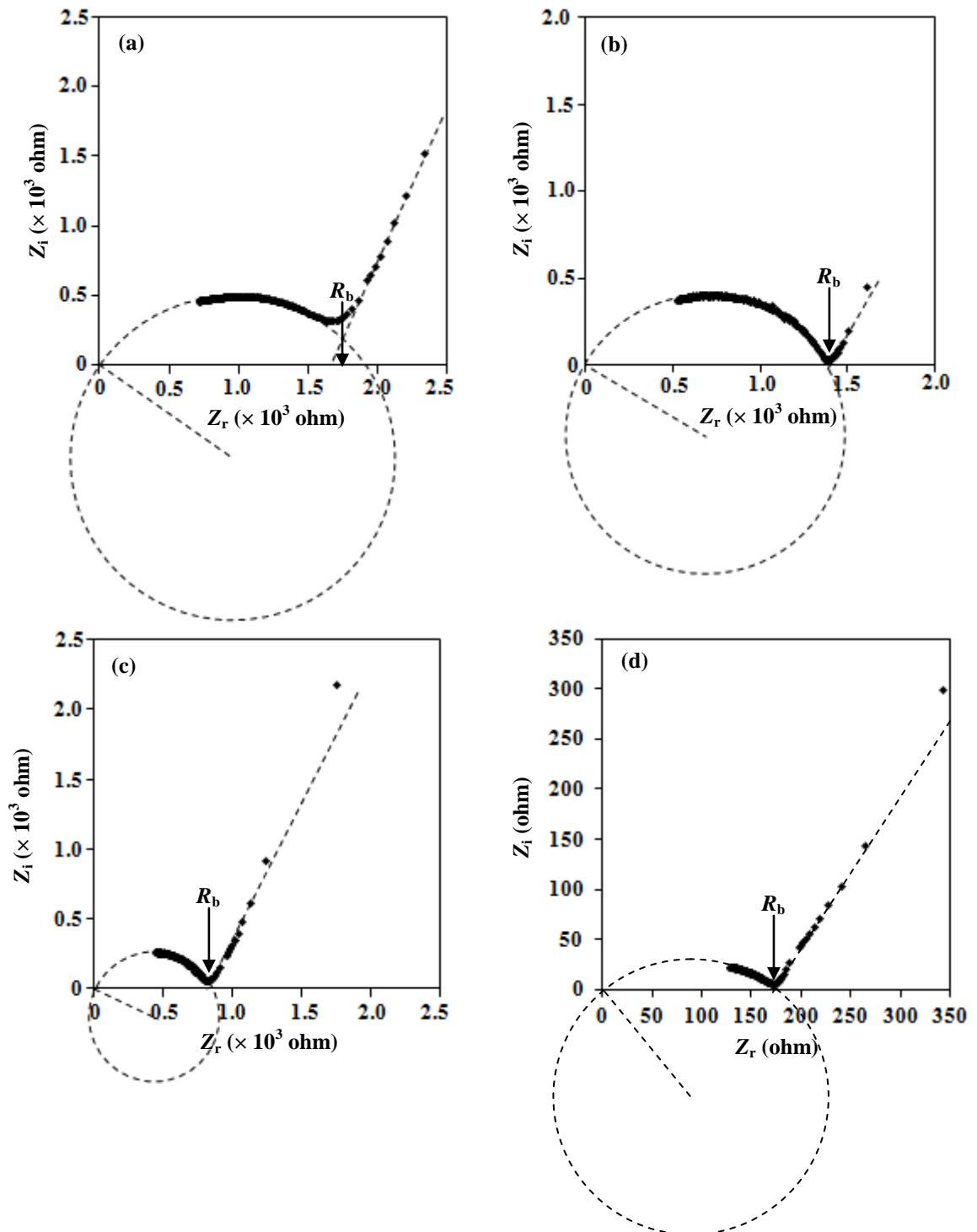


Figure 5.22 Plot of number density and mobility in PEMA/PVdF-HFP-LiTf-BMII system

## 5.4.2 PEMA/PVdF–HFP–LiTf–BMITf System

### 5.4.2.1 Composition Dependence Conductivity Studies

For this system, the ionic conducting species are  $\text{Li}^+$  and  $\text{Tf}^-$  ions from LiTf salt and also  $\text{BMI}^+$  and  $\text{Tf}^-$  ions which are contributed by BMITf. The Nyquist plots of the samples in the (PEMA/PVdF–HFP)–LiTf–BMITf system are shown in Figure 5.23.



(Figure 5.23, continued)

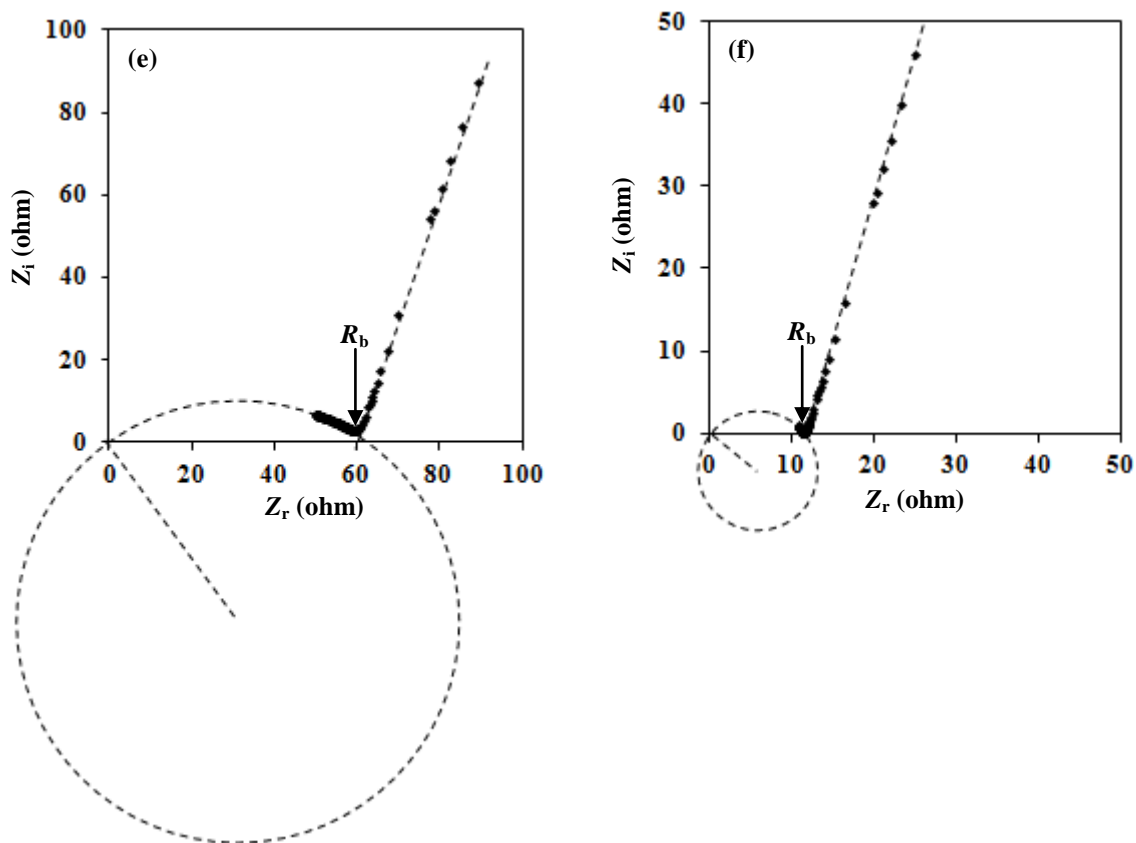


Figure 5.23 Nyquist plots of (a) BT-10, (b) BT-20, (c) BT-30, (d) BT-40, (e) BT-50 and (f) BT-60 films

Figure 5.23 (a) to (f) show a tilted incomplete semicircle at high frequencies with a spike at low frequencies for samples loaded with up to 60 wt.% BMITf. The magnitude of  $R_b$  obtained was observed to decrease when the content of BMITf was increased from 10 to 60 wt.%. Figure 5.24 shows the log conductivity plot of polymer electrolyte films added with various BMITf content. The ionic conductivity was observed to increase continuously with incorporation of BMITf up to 60 wt.%; the highest  $\sigma$  was obtained in BT-60 at  $8.59 \times 10^{-5} \text{ S cm}^{-1}$ , which was two orders of magnitude higher than BT-0 sample.

Phase separation was observed in polymer electrolyte films containing BMITf contents above 60 wt.% and hence were not considered for characterization purposes. Loss of mechanical strength with increasing amounts of ionic liquid-based polymer

electrolyte films was also reported by Singh et al. (2009) and Tang et al. (2008) in 1-ethyl-3-methylimidazolium trifluoromethanesulfonate (EMITf)-added PEO-NaI-I<sub>2</sub> and BMIBF<sub>4</sub>-added copolymer of acrylonitrile (AN), methyl methacrylate (MMA) and poly(ethylene glycol) methyl ether methacrylate (PEGMEMA), respectively. The ionic conductivity values of BMITf-added samples are listed in Table 5.10.

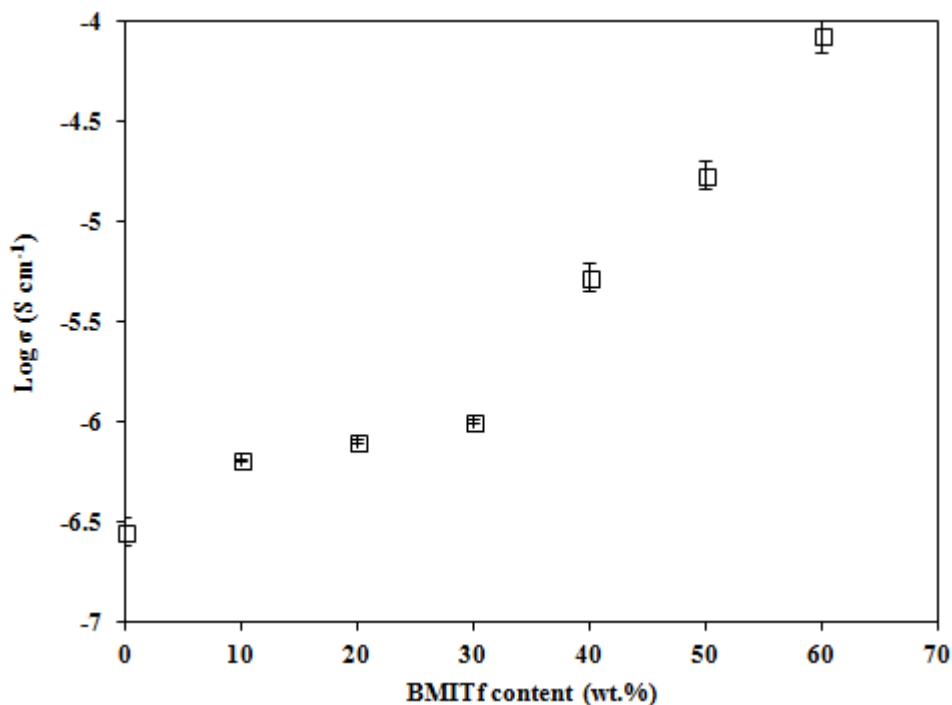


Figure 5.24 Plot of  $\log \sigma$  vs BMITf content at 298 K

#### 5.4.2.2 Temperature Dependence Conductivity Studies

The Nyquist plots of the best conducting sample of this system, BT-60 at various temperatures up to 353 K are shown in Figure 5.25. The  $R_b$  value was observed to decrease from 298 K to 353 K. Plots of  $\log \sigma$  vs  $1000/T$  for PEMA/PVdF-HFP-LiTf containing varied amounts of BMITf are shown in Figure 5.26. The temperature-dependent conductivity plots of BMITf-incorporated samples exhibit linearity which suggests Arrhenius-like behavior. The  $E_a$  values tabulated in Table 5.6 were found to decrease with increasing BMITf content, which follows the conductivity trend. The best

conducting sample in this system, BT-60 exhibits the lowest  $E_a$  of 0.15 eV. The activation energies of PEMA/PVdF-HFP-LiTf-BMITf system are listed in Table 5.10.

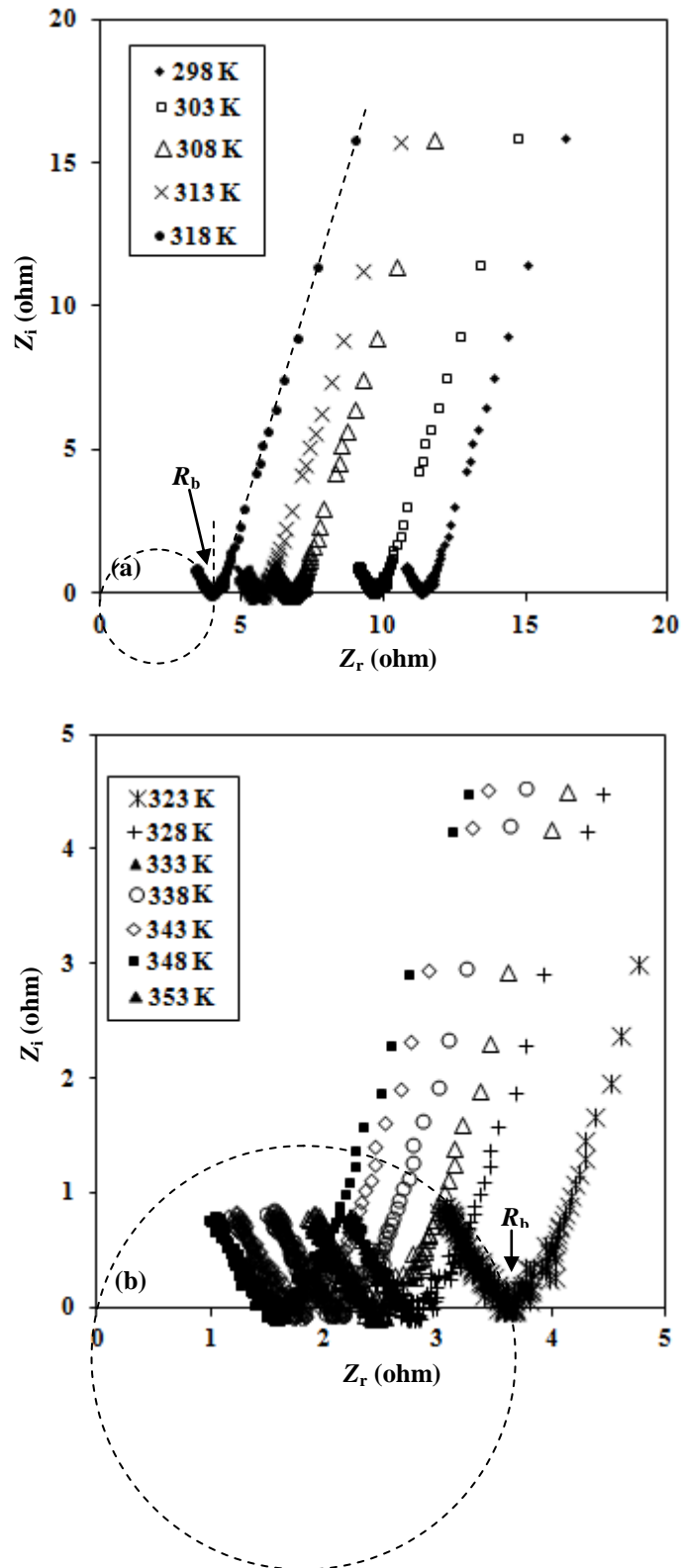


Figure 5.25 (a) and (b) Nyquist plots of BT-60 at various temperatures

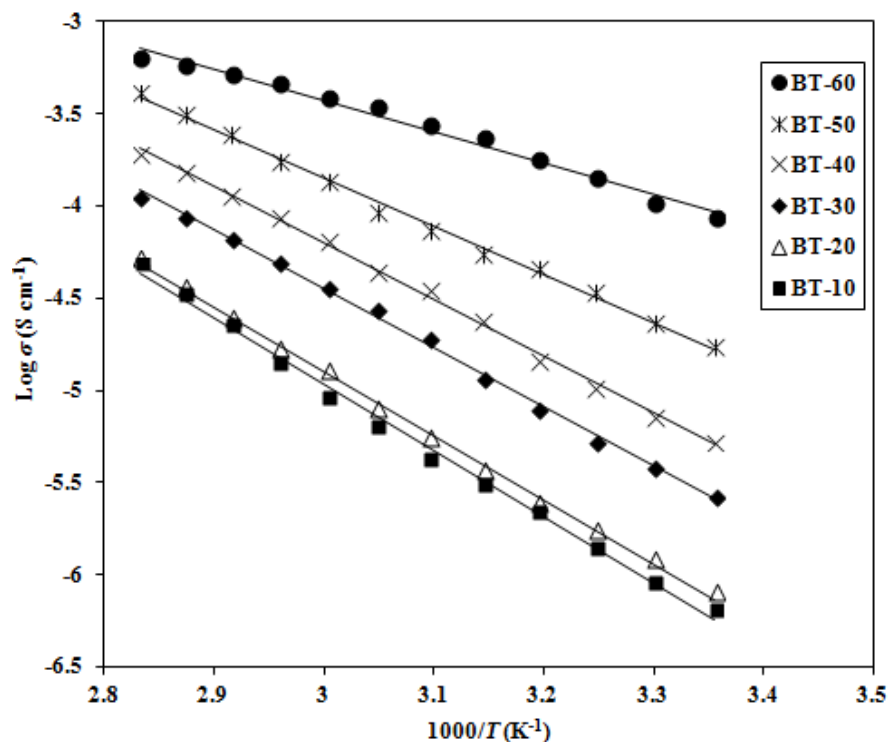


Figure 5.26 Plot of  $\log \sigma$  versus  $1000/T$  of PEMA/PVdF-HFP-LiTf-BMITf polymer electrolytes

Table 5.10 Ionic conductivities,  $\sigma$  of PEMA/PVdF-HFP-LiTf blend films incorporated with different BMITf contents at 298 K

Sample	Average $R_b$ (ohm)	$\sigma$ at 298 K ( $S\ cm^{-1}$ )	Standard error ( $S\ cm^{-1}$ )	$E_a$ (eV)
BT-10	1720	$6.50 \times 10^{-7}$	$\pm 9.10 \times 10^{-9}$	0.31
BT-20	1395	$8.05 \times 10^{-7}$	$\pm 3.90 \times 10^{-8}$	0.30
BT-30	901	$1.00 \times 10^{-6}$	$\pm 4.41 \times 10^{-8}$	0.28
BT-40	175	$5.32 \times 10^{-6}$	$\pm 2.12 \times 10^{-6}$	0.26
BT-50	61.4	$1.72 \times 10^{-5}$	$\pm 4.02 \times 10^{-6}$	0.22
BT-60	11.6	$8.59 \times 10^{-5}$	$\pm 1.60 \times 10^{-5}$	0.15

For BMITf-added system, the % area of free  $Tf^-$  ions obtained from deconvolution as listed in Table 5.11 come from the  $Tf^-$  present in LiTf and BMITf. The data used to calculate  $n$ ,  $\mu$  and  $D$  values for this system is listed in Appendix E. The plot of number density and mobility of free ions versus BMITf content is shown in Figure 5.27. The results are listed in Table 5.11. The value of  $n$  increased with addition of BMITf until 60 wt.%. The ion mobility,  $\mu$  was observed to increase significantly from  $1.02 \times 10^{-10}$  to  $3.47 \times 10^{-9}\ cm^{-2}V^{-1}s$  with increasing BMITf content.



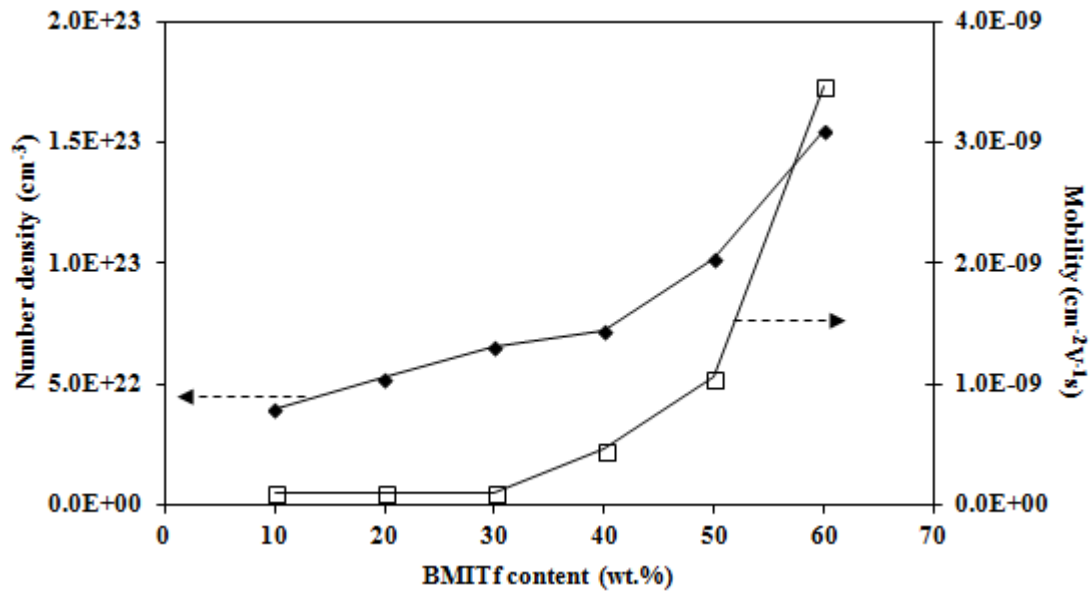


Figure 5.27 Plot of number density and mobility in PEMA/PVdF-HFP-LiTf-BMITf system

Table 5.11 Number density,  $n$ , mobility,  $\mu$  and diffusion coefficient,  $D$  of free ions for PEMA/PVdF-HFP-LiTf-BMITf system

Sample	Area of free Tf <sup>-</sup> ions of LiTf and BMITf (%)	$n$ (cm <sup>-3</sup> )	$\mu$ (cm <sup>2</sup> V <sup>-1</sup> s <sup>-1</sup> )	$D$ (cm <sup>2</sup> s <sup>-1</sup> )	$n\mu$ (cmV <sup>-1</sup> s <sup>-1</sup> )
BT-10	23.4	$3.98 \times 10^{22}$	$1.02 \times 10^{-10}$	$2.40 \times 10^{-12}$	$4.06 \times 10^{12}$
BT-20	28.4	$5.27 \times 10^{22}$	$9.54 \times 10^{-11}$	$2.24 \times 10^{-12}$	$5.02 \times 10^{12}$
BT-30	32.6	$6.56 \times 10^{22}$	$9.51 \times 10^{-11}$	$2.24 \times 10^{-12}$	$6.24 \times 10^{12}$
BT-40	33.3	$7.22 \times 10^{22}$	$4.60 \times 10^{-10}$	$1.08 \times 10^{-11}$	$3.32 \times 10^{13}$
BT-50	43.7	$1.02 \times 10^{23}$	$1.05 \times 10^{-9}$	$2.47 \times 10^{-11}$	$1.07 \times 10^{14}$
BT-60	61.7	$1.55 \times 10^{23}$	$3.47 \times 10^{-9}$	$8.16 \times 10^{-11}$	$5.36 \times 10^{14}$

## 5.5 Summary

The ionic conductivities of PEMA/PVdF-HFP-LiTf system was optimized at 30 wt.% LiTf at  $2.87 \times 10^{-7}$  S cm<sup>-1</sup>. Using this optimized polymer blend-salt composition, EC-, PC-plasticized and BMII-, BMITf ionic liquid-based polymer electrolyte systems were prepared.

- The best conducting polymer electrolyte in the plasticized and ionic liquid added system arranged in increasing order is as follows:

PC-6 ( $1.46 \times 10^{-6} \text{ S cm}^{-1}$ ) < BI-12.5 ( $4.86 \times 10^{-5} \text{ S cm}^{-1}$ ) < BT-60 ( $8.59 \times 10^{-5} \text{ S cm}^{-1}$ ) < EC-6 ( $1.05 \times 10^{-4} \text{ S cm}^{-1}$ ).

- PEMA/PVdF-HFP-LiTf and the polymer electrolyte systems incorporated with BMII and BMITf obeyed the Arrhenius model while the polymer electrolyte systems containing EC and PC were found to obey the VTF model.